UNIVERSIDAD DE VALLADOLID

ESCUELA DE INGENIERIAS INDUSTRIALES

Grado en Ingeniería Química

Conversión hidrotermal de biomasa en bioproductos valiosos

Autor:

García Riesco, Luis Miguel

RIB: Juan García Serna

University of Nottingham

Valladolid, Julio de 2019

TÍTULO: Hydrothermal conversion of biomass to valuable bioproducts

ALUMNO: Luis Miguel García Riesco

FECHA: 26 de junio del 2019

CENTRO: University of Nottingham

TUTOR: Professor Edward Lester

Palabras clave:

Biomasa, métodos hidrotermales, HTC, caracterización, bioproductos.

Resumen:

Los procesos hidrotérmicos son una excelente alternativa para convertir desechos de biomasa en productos de alto valor energético. El alcance de este proyecto ofrece el estudio de 5 tipos de biomasa distintos: café, madera blanca, arroz, lignina y madera negra (Zilkha).

La reacción se llevó a cabo en un reactor continúo cambiando las condiciones de presión y temperatura. El café demostró ser la materia primar de mayor rendimiento, alcanzando valores de hasta el 70% y, por el contrario, la lignina alcanzó muy bajos rendimientos, no sobrepasando el 13%.

Para analizar el bioproducto solido obtenido se realizó un análisis termogravimétrico. A partir de estos datos, se propuso un nuevo método denominado 'desplazamiento' que refleja las diferencias entre los perfiles del producto sólido logrado y la biomasa no tratada.

También se utilizaron técnicas de HPLC y MALDI-TOF-MS que demostraron mayores concentraciones en los bioproductos líquidos obtenidos según aumentaba la temperatura de reacción.

Table of contents

1. Abstract

Hydrothermal processing is an excellent alternative for converting biomass wastes into valuable products and thus ending the overconsumption of fossil fuels. The scope of this project offers the study of 5 different biomass feedstocks: coffee, white wood, rice, lignin and Zilkha black wood.

The reaction was carried out in a continuous reactor changing the temperature and pressure conditions. Both solid and liquid products were analysed afterwards. The highest yields were achieved from spent coffee, reaching values up to 70% and, on the contrary, lignin proved to be the most resistant material to carbonization, not surpassing yields higher than 13% even at the most extreme reaction conditions.

TGA was performed in order to analyse the solid product remaining inside the reactor. Besides the DTG profiles, from TGA data a new method was proposed called 'displacement', in order to describe the differences between untreated biomass and the biomass after reacting at different conditions. The largest displacements were observed working with coffee and the smallest with lignin, the same behaviour that yields predicted. HPLC was used to characterize the liquid product. Some similarities have been found between the reaction temperature and the number of compounds and concentrations obtained in the chromatograms. MALDI-TOF-MS analysed the dried liquid sample and the spectrum represent a molecular weight distribution related to the reaction temperature.

2. Introduction

Over the past few years the energy demand has been markedly increasing due to the fast industrialization and the notable increase of the global population. Since the fuel fossils, such as oil, coal and natural gas are running out and causing a significant environmental pollution it is required to study alternative and harmless routes of energy production, thus, many researchers have started betting on biomass as an emergent raw material.

Biomass refers to biological matter from plants or animals and their derived residues that has solar energy stored inside. It is deemed to be a potential energy source and is

considered to be inexpensive, clean, and environmentally friendly (Kumar, Olajire Oyedun, & Kumar, 2018).

One of the advantages of biomass is that appears as renewable source and some diverse methods have been found to be profitable and, at the same time, respectful with the environment, as biomass is considered to be CO_2-neutral and therefore plays of a role in CO_2 reduction strategies (Lester et al., 2018), taken from the atmosphere by plants through photosynthesis, is utilized by the plant as a source of energy and returned to the atmosphere without additional CO2 release (Tekin, Karagöz, & Bektaş, 2014).

However, there are disadvantages to biomass as sustainable resource that urgently need to be overcome; for examples, its high moisture, low energy content, heterogeneity, low density, and presence of contaminants (Wang, Zhai, Zhu, Li, & Zeng, 2018). The main problem with the high moisture is basically economical since a significant amount of energy would be needed for the drying processes.

One of the ways to take advantage of the full potential that biomass has is through hydrothermal processes. Hydrothermal conversion of biomass in hot-compressed water is a viable, scalable, and energy-efficient thermo-chemical route for converting biomass into a synthetic solid, liquid, or gaseous fuels and chemicals (Pedersen et al., 2016). The process also leads to by-products that can be used for power generation and the recovery of useful nutrients (Kumar et al., 2018).

The conversion of the biomass is carried out by several complex reactions depending on the physical properties of the water. These properties are usually manipulated changing the temperature, pressure and the time of the reaction in order to obtain the desired products. There is such an extensive classification for the different hydrothermal methods but in this report, only the 3 most important technologies will be described:

- <u>Hydrothermal carbonization (HTC)</u>

They hydrothermal carbonization is a thermochemical process for the pre-treatment of high moisture content biomass to make it viable in several applications (Heidari, Dutta, Acharya, & Mahmud, 2018). HTC is performed under subcritical water conditions, in a range of temperature usually between 180-350ºC under a pressure between 550-1150 psi during 4h in a Batch reactor (Arellano et al., 2016).

This method is used to convert the lignocellulosic materials into solid hydrochars, which have better physiochemical characteristics than the raw biomass feedstock (Álvarez-Murillo, Sabio, Ledesma, Román, & González-García, 2016), but also the liquid product can be characterized for chemical composition. Fig. 1 provides a global vision of the reaction pathways and the key products of the hydrothermal carbonization.
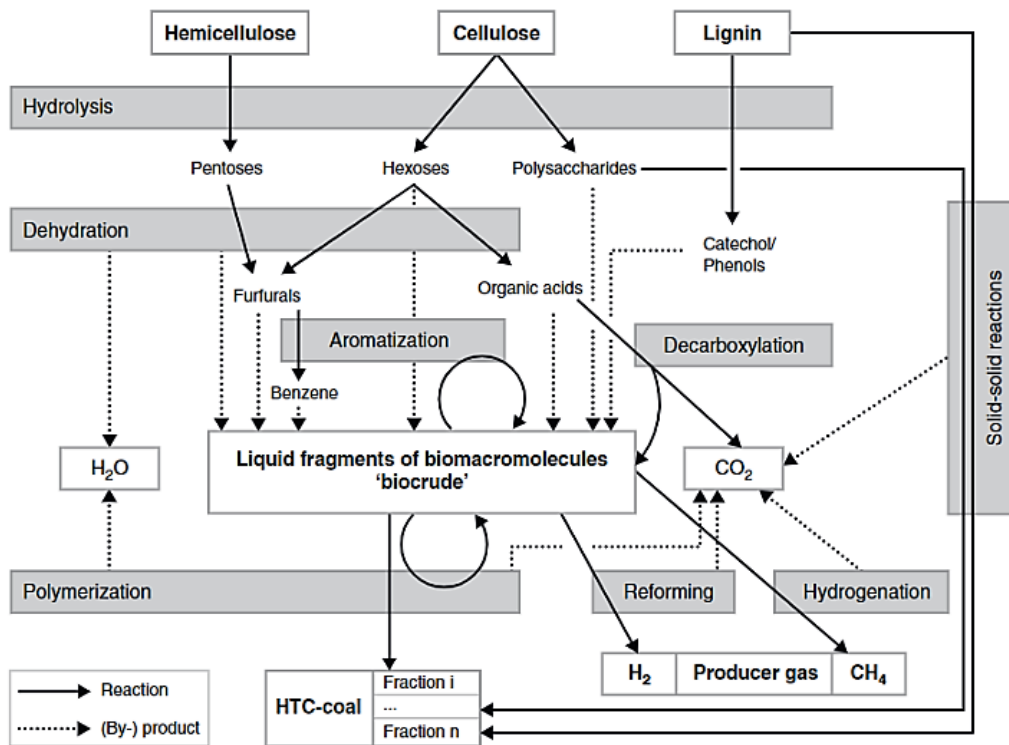

Fig. 1. Reaction pathways of hydrothermal carbonization (Adapted from: Kruse, Funke, & Titirici, 2013).

Large and useful applications of the hydrothermal carbonization has been found in recent years, such as the thermal conversion of the municipal waste water into sterilized value-added hydrochar (Berge et al., 2011) or even in biolectrochemical components from the synthesis of a microcellular electrode material by the hydrothermal carbonization (Flexer et al., 2016).

▪ Hydrothermal liquefaction (HTL)

The hydrothermal liquefaction is the wet processing route where the feedstock is processed at high temperatures, usually between 250-350ºC and pressures about 5-24 MPa and it can be carried out with or without catalysts to produce an upgradable biocrude fraction (Cherad, Onwudili, Biller, Williams, & Ross, 2016).

The HTL is suitable for the fuels production from high moisture biomass, such as seaweed, sewage sludge or microalgae, since it involves the direct conversion of the biomass into liquid in the presence of a solvent, therefore saves the high costs of the drying/dewatering step (Dimitriadis & Bezergianni, 2017).

Several complex reactions take place during the transformation of the biomass feedstock into crude oil like products (Gollakota, Reddy, Subramanyam, & Kishore, 2016), however, in Fig. 2 there are some recurrent steps that occurs along the process depending on the initial molecule.
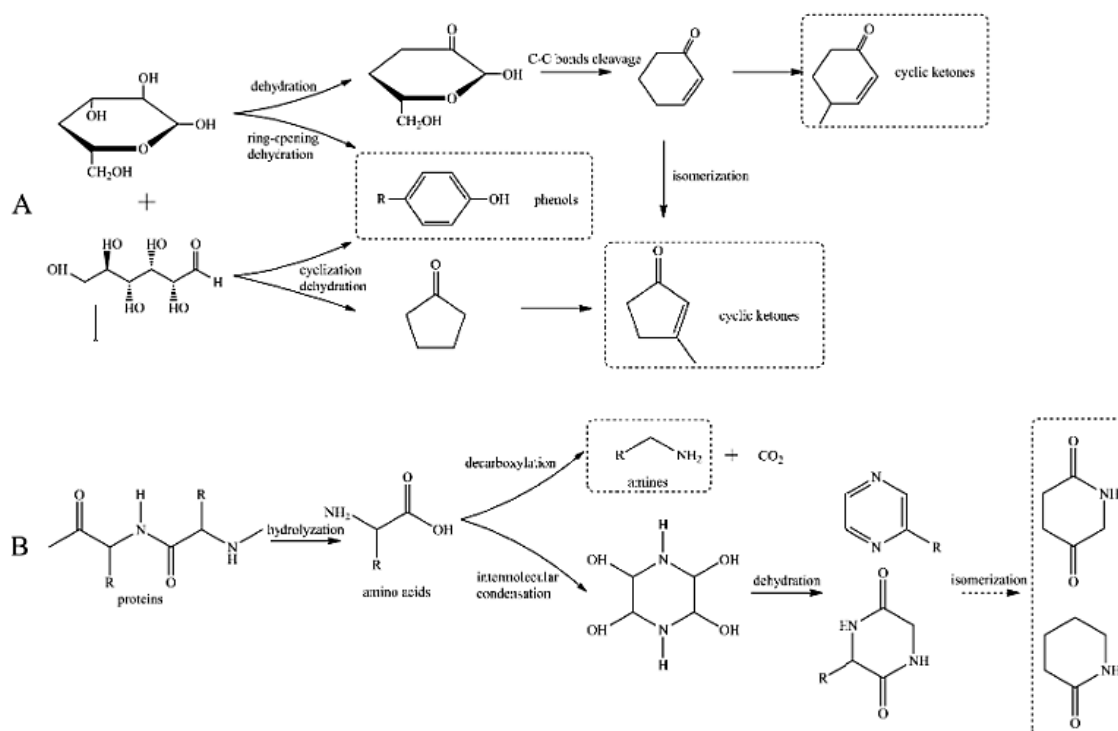

Fig. 2. Possible conversion pathways of (A) polysaccharides and (B) proteins into bio-oils through hydrothermal liquefaction (Adapted from: Yang, Li, Li, Tong, & Feng, 2015).

- <u>Hydrothermal gasification (HTG)</u>

The hydrothermal gasification is a reaction that is carried out with a temperature higher than 350ºC in the absence of oxidants with the aim of producing a flue gas rich in either CH_4 or H_2 depending on the conditions of the reaction (Cherad et al., 2016). Fig. 3 provided insight into the reaction pathways and expected products for the HTG.

The main product expected to obtain with this technology is called "syngas" which predominantly contains CH_4, H_2, CO_2 and CO, but also may contain a significant amount of undesirable impurities that reduce the energy value of the syngas. This impurities are

composed of tars, sulphur compounds, such as SO_2; nitrogen compounds, such as NH_3 and HCN; hydrogen halides, such as HCl and HF and some trace of various metals (Abdoulmoumine, Adhikari, Kulkarni, & Chattanathan, 2015).
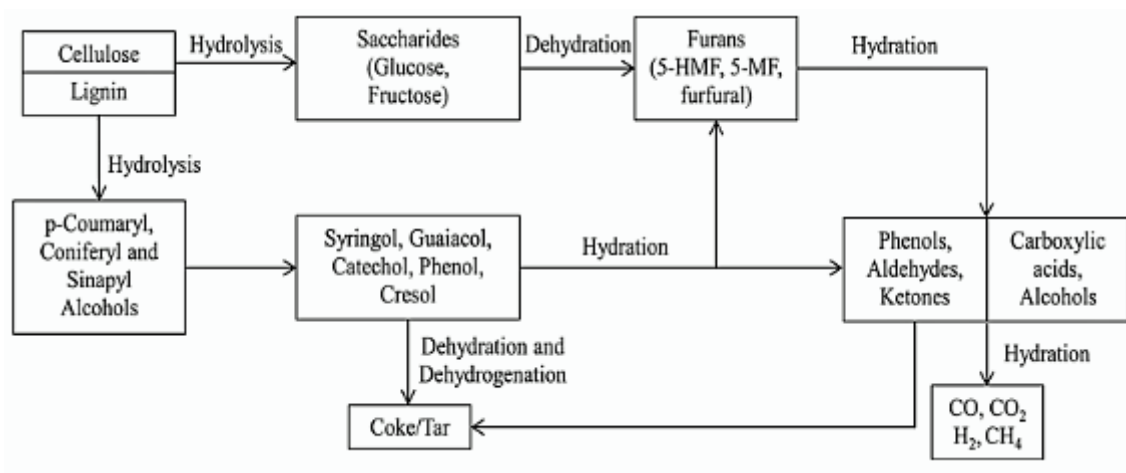

Fig. 3. Simplified mechanism for conversion of lignocellulosic materials through hydrothermal gasification (Adapted from: Güngören Madenoğlu, Sağlam, Yüksel, & Ballice, 2016).

The reduction of tars has been explored in the last years due to it is the key to improve the calorific power of the syngas generated and, consequently, could make this technology unsuccessfully from a commercial point of view. There are two ways to overcome this problem: The optimization of the operation conditions, such as temperature, pressure, vapor fraction etc., or the tar removal at the gas outlet subsequently in the post-gasification treatments (Valderrama Rios, González, Lora, & Almazán del Olmo, 2018).

3. Materials and methods

All the biomass materials and the solvent utilized for this research project are described below in addition of the methods and technologies used for the product characterization.

3.1. Solvent

Since this project is about hydrothermal methods the only solvent used on all of the experiments was water, specifically, distilled water.

The water is the most common, easy handling and environmentally innocuous medium for organic reactions. It can be found as solid, liquid or gas depending on the conditions. Beyond the critical point (T_c = 374°C, P_c = 22,06 MPa) the water behaves as a

supercritical fluid, this means that properties such as density, dielectric constant, viscosity, etc. show very different variations with the other phases. These properties make the water an excellent solvent for almost all of the organic reactions due to the high miscibility that it presents in the supercritical phase. Fig. 4 show, as an example, the isobaric changes for the dielectric constant when it reaches the critical temperature. The big decrease of the dielectric constant is due to the water dissociation in OH^- and H^+ ions, also the ionic product, K_w, drops sharply beyond 300ºC (Perlt, von Domaros, Kirchner, Ludwig, & Weinhold, 2017).
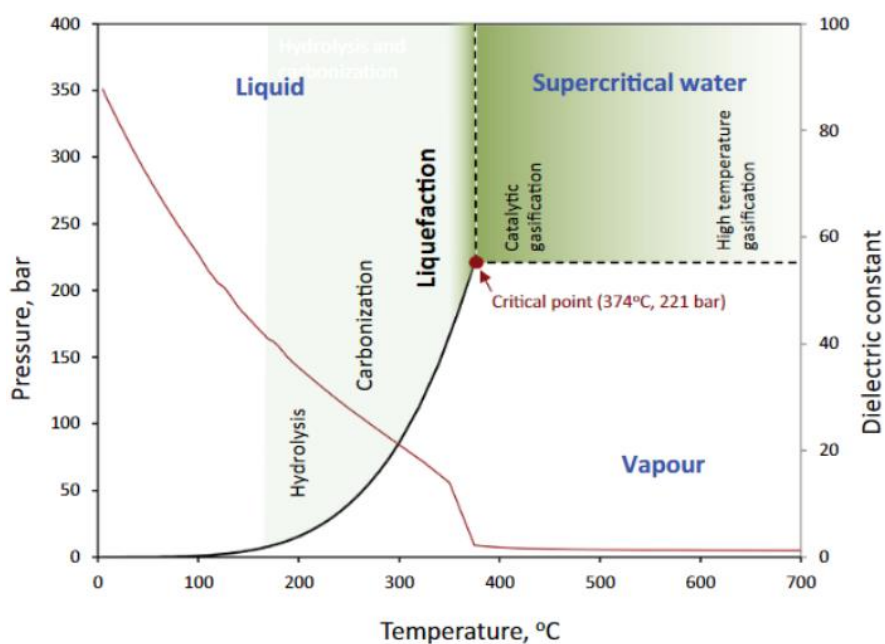
Fig. 4. Phase diagram of water at different temperatures and pressures with the static dielectric constant at 200 bar as a function of the temperature (Adapted from: Tran, 2016).

During the hydrothermal treatments water has different roles, first acting as a solvent but also as a reactant and catalyst in all the hydrolysis reactions that take place in the reactor.

However, despite the water acts as a superb solvent, other organic solvents have been also examined such as methanol and ethanol, these technologies are called "solvothermal methods", since the water is not involved. It is important to note that the critical points of methanol (239ºC, 8.08 MPa) and ethanol (241ºC, 6.3 MPa) are much lower than those that were mentioned for water (334ºC, 22,06 MPa), while they also have a lower dielectric constant compared to water and boiling point (Dimitriadis & Bezergianni, 2017). This implies that less energy will be needed in the processes that use methanol or ethanol as solvent instead of water.

All these advantages make methanol and ethanol promising solvents for solvothermal liquefaction and the production of valuable bioproducts, and it has been proven that these solvents can reach higher yields than water (Singh, Bhaskar, & Balagurumurthy, 2015).

Nevertheless, the opposite behaviour was shown on the liquefaction of pine sawdust, where the highest conversion and bio-oil yield for the same temperature (300ºC) were obtained at with a co-solvent of 50 wt % aqueous alcohol (methanol or ethanol) than those for mono-solvent, whether alcohol or water (Cheng, D'cruz, Wang, Leitch, & Xu, 2010).

3.2. Biomass composition

All biomass materials are composed of 5 chemical elements: carbon (C), hydrogen (H), oxygen (O), nitrogen (N) and sulphur (S). The most relevant element is the carbon due to it represents the major contribution to the overall heating value. During the combustion, it is converted into CO_2 that is discharged into the atmosphere (Gollakota, Kishore, & Gu, 2018). In point of fact, the number of these elements does not give enough information about the properties of the material, it is more successful to look into the bigger structures.

Biomass is divided into different types: lignocellulosic biomass (wood, straw, etc.), aquatic biomass (microalgae, seaweeds, etc.) and fresh biomass (leaves, grass, etc.). Each type of biomass has different number of components, but in this project, only the lignocellulosic group is going to be developed.

The lignocellulosic biomass is mainly composed in lignin, the non-carbohydrate source; cellulose and hemicellulose, the carbohydrate sources; but also it contain lipids and proteins that constitute the wet biomass feedstock (Gollakota et al., 2018). These components will be explained in more detail below:

3.2.1 Lignin

Lignin is a natural polymer made up of aromatic blocks that are cross-linked by carbon and ether linkages. It is an amorphous material, considered as hydrophobic since its solubility in water is very low. Lignin makes up 15-35% of the lignocellulosic materials and is the largest renewable source of aromatics (Jensen et al., 2018).

Lignin molecules are highly relevant in the formation of cell walls, especially in materials like wood and bark, because they provide rigidity to the whole and therefore, they do not break easily. Compared with the rest of bioorganic compounds listed below, lignin is the most resistant to natural decay and biological degradation. A major lignin content

provides a biomass feedstock with a higher heating value owing to the higher energy content of lignin in comparison with those of hemicellulose and cellulose. (Vassilev, Baxter, Andersen, Vassileva, & Morgan, 2012).

The yield achieved during the hydrothermal processing fairly depends on the structure that lignin presents. Lignin components are usually depolymerized through a series of reactions that involves degradation and re-localization, the degree of which depends on the process conditions. The mainly products that results from this degradation are phenolic compounds with ethyl and methyl groups (Savage, Levine, & Huelsman, 2010).

3.2.2 Cellulose

Cellulose is an organic compound usually represented by the generic formula $(C_6H_{10}O_5)_n$ which supposes a mass content of 44,4% carbon, 6,2% hydrogen and 49.4% of oxygen. Cellulose is a long chain polysaccharide of β-(1→4)-D-glucopyranose units with a high degree of polymerization, around 10.000 units, and a large molecular weight (Álvarez-Murillo et al., 2016). Fabrics as cotton are composed by around 90% of cellulose, while wood biomass have usually about 40-50% content of cellulose.

The solubility of cellulose in water at room temperature is negligible at room temperature but it starts being soluble above 300ºC and completely soluble at 330ºC under subcritical water conditions (Tekin et al., 2014), due to the action of hydroxyl (OH^-) and hydronium (H^+) ions.

Cellulose can be efficiently converted into bio-oil through two step approaches: an ultrasonic pre-treatment that destroys the physical structure of cellulose facilitating its solubility in water followed by liquefaction in hot-compressed water. This pre-treatment increases significantly the conversion of the cellulose and therefore, the bio-oil yield (Shi, Li, Jia, & Zhao, 2013).

3.2.3 Hemicellulose

Hemicellulose is an amorphous heteropolysaccharide related to cellulose that forms approximately 20-30% of the dry weight of most wood species but in herbaceous or agricultural biomasses the amount is quite lower. The hemicellulose structure varies depending on the biomass source (Tekin et al., 2014), usually built up of D-xylopyranose, L-arabinofuranose, D-glucopyranose, D-mannopyranose and D-galactopyranose monomers. It has a lower degree of polymerization than cellulose, it is approximately 100-200 per each hemicellulose molecule.

Hemicellulose, forms hydrogen bonds with cellulose and at the same time it forms covalent bonds with lignin (primarily α-benzyl ether bonds), and ester bonds with hydroxycinnamic acids and acetyl units. All these different bonds make the hemicellulose more unstable than cellulose and therefore, it is more easily degradable when subjected to hydrothermal treatments.

3.2.4 Proteins

A protein is a large biomolecule that consist of one or more long chains of amino acids. Amino acids are valuable products used as food additives in the nutrition (human and animal) but also used in the pharmaceutical and cosmetic sectors. In turn, peptides are formed by a long chain of proteins.

The recovery of amino acids from protein of animal waste biomass has been carried out by some researchers through hydrothermal methods. The first step was the degradation of the raw material feedstock and the formation of glucose with the hydrolysis of protein to amino acids. In the next step, these primary unstable products suffer a second degradation that result in the formation of carboxylic acids (acetic acid, propionic acid, n-butyric acid, etc.), phenols, furfurals and carbohydrates (Pińkowska & Oliveros, 2014).

Proteins are one of the major constituents in the algal biomass, such as seaweed or microalgae. For this reason, microalgae are widely used in hydrothermal liquefaction due to it reaches high biocrude oil yields (Li et al., 2014).

3.2.5 Lipids

A lipid is a natural molecule that is soluble in nonpolar solvents (typically hydrocarbons), this also means they are hydrophobic, immiscible in water. These similarities with aliphatic compounds are due to the majority of the lipids are made up of hydrocarbon chains, such as the triglycerides (TAG's, also called fats) composed by three esters of fatty acids along with a glycerol molecule.

Fresh biomass, as microalgae, generate a wide range of lipids including hydrocarbons, polar lipids, neutral lipids, wax esters, sterols, and prenyl derivatives such as terpenes, carotenoids, quinines, tocopherols and pyrrole derivatives such as chlorophylls (Sajjadi, Chen, Raman, & Ibrahim, 2018).

At room temperature, the fats are mainly insoluble in polar solvents but gradually tends to be soluble with the change in temperature, the same behaviour can be seen as in of

cellulose. Furthermore, the dielectric constant of the solvent, as water for example, at the sub-critical conditions allows higher miscibility (Peterson et al., 2008).

During hydrothermal liquefaction, glycerol is not turned into any oily phase, it turns to be soluble in water instead. Moreover, the glycerol degradation leads to a product stream of formaldehyde, acetaldehydes, propionaldehyde, ethanol, allyl alcohol, acrolein, CO, CO_2 and H_2 (Gollakota et al., 2018).

3.3. Biomass raw materials

In this research project, 5 different types of biomass have been studied:

Coffee. Obtained from coffee machine capsules that were already used. The spent coffee powder was extracted from the capsules and left on filter paper at room temperature for a few days.

White wood. Obtained from sawdust of white wood.

Rice. Obtained from rice pellets that were ground into powder.

Lignin. Obtained from lignin pellets that were ground into powder.

Zilkha. Obtained from Zilkha Black® pellets that were ground into powder.

All of the materials were first sieved to obtain a size particle more than 200 micrometres before starting the experiments.

3.4. Process flow diagram

This research Project has been carried out in one of the rigs at laboratory B05 in L3 building within the Chemical and Environmental Engineering department of the University of Nottingham.

In Fig. 5 the process flow diagram (PFD) of the rig has been represented. The operation of the rig consists of a semi-continuous reactor that works by loads. The feed stream is driven from a distilled water tank (TK-101) with the aid of a peristaltic pump (P-101) and is preheated to the desired temperature in an electric heater (E-101). Subsequently, the water stream is introduced to the reactor (R-101) from the bottom, where the reaction starts by the effects of matter and energy transfer. The enriched stream leaves the reactor and passes through a filter (F-101) of 200 micrometres that retains the possible solids that have been able to escape from the reactor. After the filter, the resulting products are cooled in a heat exchanger (E-102) with a stream of fresh water. Finally, the product

stream goes through a back-pressure regulator (BPR) which is the valve that is responsible for pressurizing the entire process line. The product stream is collected after the BPR in sample cans (TK-102) for further analysis.
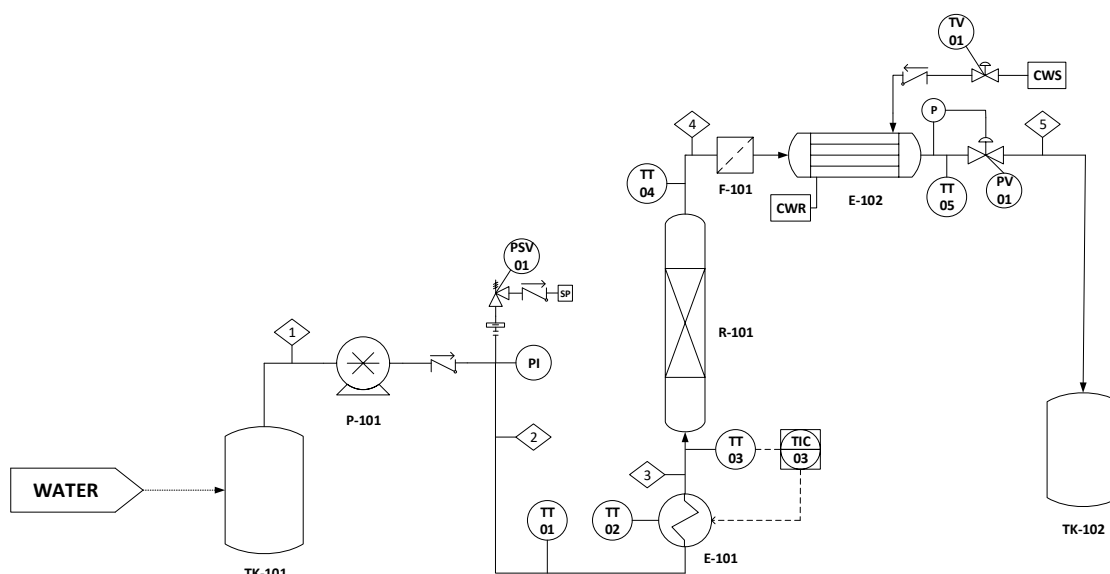
Fig. 5. Process flow diagram of the rig.

3.5. Operating conditions

In each experiment the reactor is loaded with 5 grams of the material to be explored. This reactor works as a fluidized bed, placing at the ends two metallic filters that do not allow the pass of solids.

The flow rate of distilled water was set at 20 ml/min for all of the experiments. This is the normal flow rate due to the capacity of this rig.

According to the purpose of this study, the experiments were carried out at 4 different temperatures to make a comparison of the results obtained in each of them. Previously, a check of the thermocouples on the rig was made in order to verify that they worked correctly. Table 1 shows the temperatures at different set points of the controller.

Table 1
Check of thermocouple temperatures (ºC).

Thermocouple	25 ºC	100 ºC	180 ºC	300 ºC
TT-01: Heater block	41.8	108.7	178.2	281.4
TT-02: Bottom of reactor	38.6	84.7	141.3	215.1
TT-03: Top of reactor	20.7	44.9	98.7	165.1
TT-04: Precooler	20.1	40.4	88.8	148.6
TT-05: Post cooler	20.4	19.6	18.9	28.6

The temperatures chosen to carry out the experiments were 25ºC, 75ºC, 150ºC and 250ºC. This range of temperature is typical of the hydrothermal carbonization, as seen in the introduction, so it is expected to obtain similar results to those of the literature.

Following the same purpose, 3 different operating pressures were set for each temperature: 1 bar, 50 bar and 240 bar. The rig has a pressure safety valve set to 275 bars; it opens automatically to release the pressure if it exceeds that value.

To sum up, 12 experiments for each biomass need to be carried out to perform all of the pressures and temperatures, which means a total of 60 experiments.

3.6. Characterization methods

Some analytical methods have been used to measure the success of the experiments. In this particular study it is interesting to analyse both the product obtained in the liquid phase and the solid biomass that remains in the reactor when finished.

All the solid biomass samples were weighed at the beginning and at the end of each experiment after being dried. With this data it can be calculated the HTC-char yield that is defined in the Equation 1 according to Köchermann, Görsch, Wirth, Mühlenberg, & Klemm (2018).

$$\text{Char Yield} = \frac{m_{HTC-Char,dry}}{m_{feed,dry}} \cdot 100\% \tag{1}$$

Where $m_{feed,dry}$ is the dry matter of biomass feedstock and $m_{HTC-Char,dry}$ is the resulting dry char after each trial.

The yield can be calculated for the experiments performed at different reaction conditions.

3.6.1. TGA

Thermogravimetric analysis (TGA) was the method chosen for the characterization of the solid product. The TGA indicates how the hydrothermal treatment has hydrolysed the biomass components mentioned before (hemicellulose, cellulose and lignin).

This technique consists in analysing the behaviour in the composition of a solid sample measured over time under gasification conditions in an inert atmosphere of nitrogen to determine the carbonization (Yedro, García-Serna, Cantero, Sobrón, & Cocero, 2014).

A small amount of each sample, 15-20 mg approximately, need to be placed onto little pans that are usually heated from room temperature up to a maximum temperature of

900ºC using a heating rate of 5 ºC/min under a nitrogen atmosphere (30 ml/min). Then, the gas is changed to air at 30 ml/min in order to burn off all the fixed carbon so that it is able to determine the ash content (Lester, Gong, & Thompson, 2007).

Thermogravimetric (TG) and differential thermogravimetric (DTG) curves, the main results of TGA, are basically used to characterize the combustion and devolatilization behaviour of a biomass sample and also helps to quantify the combustion characteristics of fuel, such as degradation rate, thermal reactivity or the initial and final combustion temperatures (Ninduangdee et al., 2015).

3.6.2. HPLC

The high-performance liquid chromatography (HPLC), or also referred to as high-pressure liquid chromatography, is a type of column chromatography frequently used in biochemistry and analytical chemistry both for the identification and for the separation of components.

The HPLC technique was used in this research in order to characterize the components obtained in the liquid phase. Only 20 µl of liquid sample are injected into the column. This column works as reverse phase. The mobile phase is composed of water as aqueous solvent and acetonitrile as an organic solvent that works in gradient.

After all of the liquid samples were run, two calibration curves were elaborated by using commercial standards of the interesting compounds with known concentrations.

The two most interesting compounds are lignin and cellulose. Lignin gives information about the cell wall degradation of plant origin materials. while the cellulose gives information about the content inside the cell. Besides, both are intimately associated. The destruction of the complex lignin molecule provides the access to the cellulose moiety.

Due to the absence of lignin and cellulose standards, it was decided to carry out glucose standards that would simulate the behaviour of cellulose, since it is a β-glucose polymer, and vanillin was chosen for lignin due to the similarity of both molecules.

3.6.3. MALDI-TOF-MS

The analysis by MALDI-TOF MS (Matrix-assisted laser desorption/ionization time-of-flight with a mass spectrometry detector) has become a reference method for the identification of different chemical compounds or even the analyse of biological microorganisms (Santos, Hildenbrand, & Schug, 2016).

MALDI-TOF is a soft ionization method that can analyse materials with a high molecular weight. Nevertheless, it is impossible to identify all the components that appear in the sample because of the excessive amount of data that it gives. The purpose of this method is to draw a graph with the distribution of the molecular weight. This distribution change with the increased reaction temperature and time and can be calculated by integrating the area for each segment of the analysed MALDI-TOF spectrum (Kim et al., 2016).

MALDI requires samples to be co-crystallized with a matrix in a solid form. The matrix used was DCTB (2-[(2E)-3-(4-tert-butylphenyl)-2methylprop-2-enylidine] malonitrile), which is a nonpolar aprotic matrix used frequently in MALDI analyses.

In order to get a solid sample form, the liquid phase products obtained in each experiment were introduced in an oven to evaporate the water from the samples. The solid product that remains after evaporation is the object to be analysed with MALDI.

4. Results and discussion

4.1. Standards

In order to obtain reliable results, the standards have been performed at 7 different concentrations: 0.5 µM, 1 µM, 5 µM, 10 µM, 25 µM, 50 µM and 100 µM. The calibration curves are represented below for each component.

4.1.1. Glucose
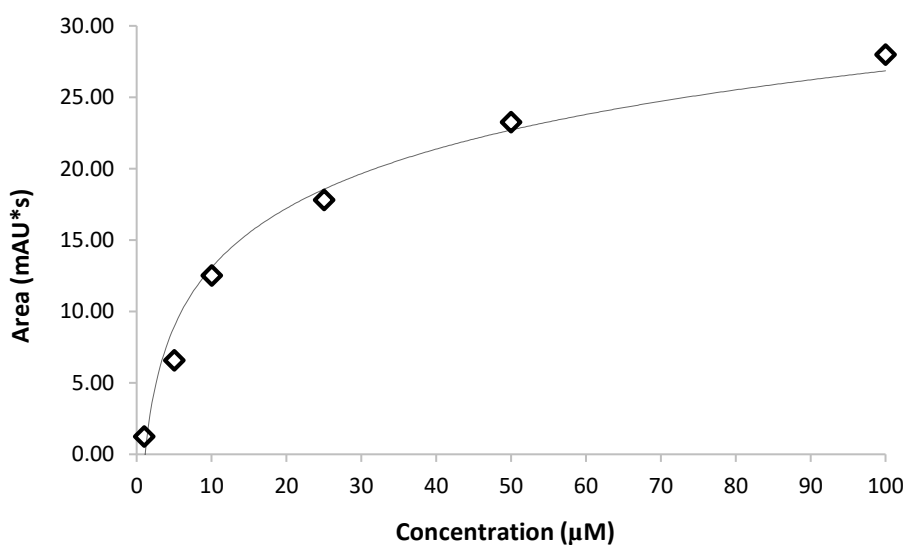
Fig. 6. HPLC calibration curve for glucose standards.

The calibration curve for glucose is displayed in the Fig. 6. The signal of the standard with the lowest concentration was practically imperceptible due to the noise produced by the solvent. The average retention time for glucose was 4.369 min.

The regression that best fits the glucose data is a logarithmic expression (Ec. 2).

$$\text{Area} = 5.9831 \cdot \ln(\text{Concentration}) - 0.7008 \tag{2}$$

4.1.2. Vanillin
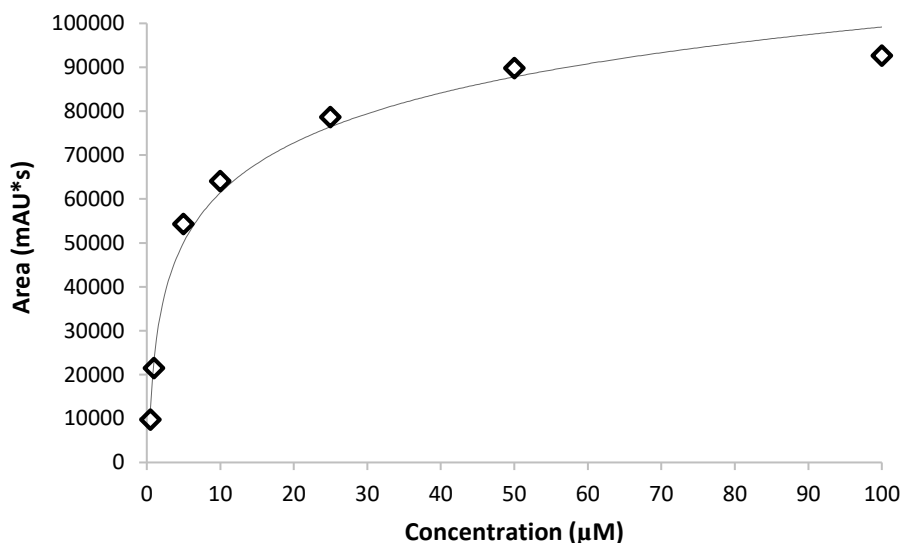
Fig. 7. HPLC calibration curve for vanillin standards.

The calibration curve for vanillin is represented in the Fig. 7. All of the standards were recognized by the column with more intensity. The average retention time for vanillin was 13.771 min.

The best regression that fits the vanillin data is also a logarithmic expression (Ec. 3).

$$\text{Area} = 16396 \cdot \ln(\text{Concentration}) + 23661 \tag{3}$$

4.2. Characterization

The data collected in the four characterization methods mentioned before is represented in the sections below showing the results obtained for each biomass feedstock.

4.2.1. Carbonization yield

- Coffee

Table 2 shows the results obtained for the char yield of coffee, resulting from Ec.1.

Table 2
Char yield of coffee experiments.

Pressure (bar)	Temperature (ºC)			
	25	75	150	250
1	2.89%	2.01%	32.65%	69.31%
50	1.42%	7.98%	12.94%	60.98%
240	2.54%	4.01%	11.55%	60.16%

Working with coffee, the highest yield (69,31%) was achieved at the highest temperature and the lowest pressure. At these conditions, the water is in vapor state (steam). Furthermore, the yields obtained at the highest temperature but with higher pressures are not far away from the highest yield.

- White wood

Table 3 shows the results obtained for the char yield of white wood, resulting from Ec.1.

Table 3
Char yield of white wood experiments.

Pressure (bar)	Temperature (ºC)			
	25	75	150	250
1	2.96%	3.82%	4.78%	21.37%
50	3.35%	4.71%	6.97%	41.15%
240	4.52%	6.96%	7.07%	41.21%

Working with white wood, the highest yield (41.21%) was achieved at the highest temperature and the highest pressure, following closely the experiment at medium pressure and high temperature.

- Rice

Table 4 shows the results obtained for the carbonization yield of rice, resulting from Ec.1.

Table 4
Char yield of rice experiments.

Pressure (bar)	Temperature (ºC)			
	25	75	150	250
1	2.16%	1.60%	9.55%	13.58%
50	1.76%	2.01%	5.85%	37.30%
240	1.20%	4.36%	7.96%	38.94%

Working with rice, the highest yield (38.94%) was achieved at the highest temperature and the highest pressure, following closely the experiment at medium pressure and high temperature as well.

- Lignin

A Table 5 shows the results obtained for the char yield of lignin, resulting from Ec.1.

Table 5
Char yield of lignin experiments.

Pressure (bar)	Temperature (ºC)			
	25	75	150	250
1	3.71%	6.70%	7.52%	10.29%
50	3.93%	4.99%	5.18%	12.35%
240	6.20%	6.30%	4.67%	7.02%

Working with lignin, all of the yields obtained were quite low, achieving the highest (12.35%) at the highest temperature and medium pressure. The yield for the experiment at highest temperature and pressure turned out to be lower than expected.

- Zilkha

Table 6 shows the results obtained for the char yield of Zilkha, resulting from Ec.1.

Table 6
Char yield of Zilkha experiments.

Pressure (bar)	Temperature (ºC)			
	25	75	150	250
1	10.21%	12.68%	17.82%	20.38%
50	10.06%	12.85%	15.91%	28.62%
240	11.07%	13.07%	14.74%	23.87%

Working with Zilkha, all of the yields obtained were quite low, achieving the highest (12.35%) at the highest temperature and medium pressure. The yield for the experiment at highest temperature and pressure turned out to be lower than expected.

To sum up, spent coffee powder achieved the highest yields and lignin powder was the biomass material that got the lowest yields.

4.2.2. TGA

In this epigraph, the weight loss differences between the experiments will be represented on TG and DTG curves.

First, the temperature gradient in all TG analyses has been represented in Fig. 8. The temperature starts increasing with a rate of 5ºC/min until reaches 900ºC, Then, it is stable for a short time to burn off the fixed carbon in the sample and then starts decreasing.
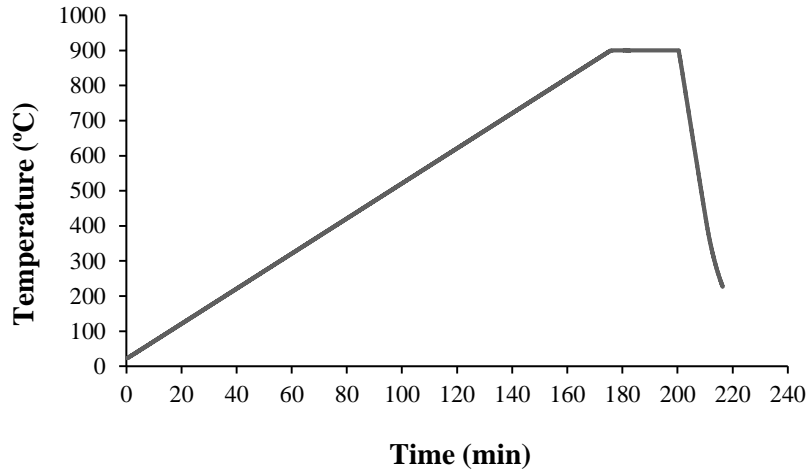
Fig. 8. Temperature gradient as a time function.

Next, in Fig. 9 and Fig. 10 show the TG and DTG curves respectively for the biomass raw materials without being treated.
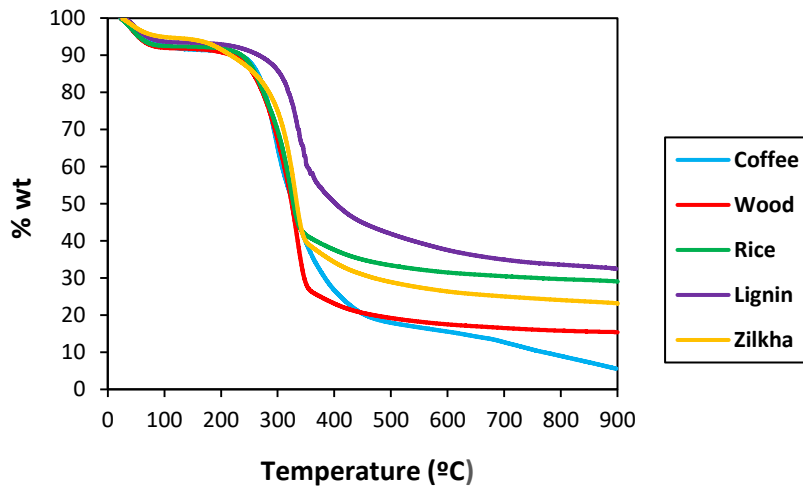
Fig. 9. TG profiles for raw biomass feedstocks.
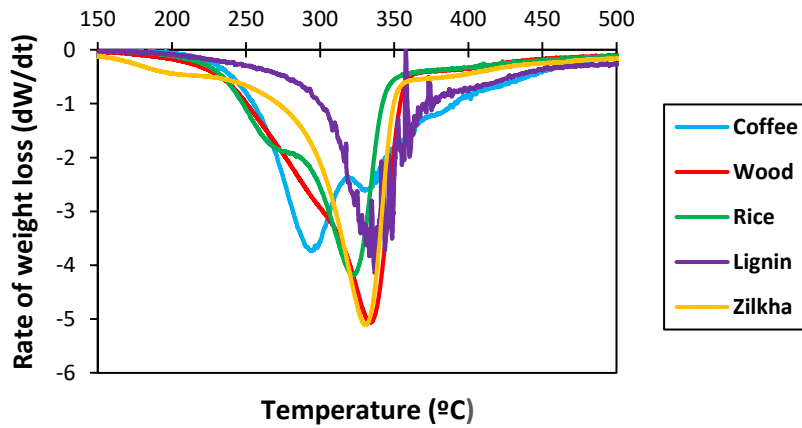
Fig. 10. DTG profiles for raw biomass feedstocks.

It can be seen in Fig. 9 that the TG profile for lignin is the highest curve, which means that is the biomass with the largest amount of fixed carbon and as coffee is the lowest curve, it has also the shortest amount of fixed carbon. Similar behaviour is showed in Fig. 10 through the DTG profile where the lignin peak is the most displaced to the right and the opposite occurs for coffee. This main peak represents the devotalization temperature.

As it can be appreciated, these displacements are also related with the yields these materials achieved. In conclusion, the less amount of fixed carbon the higher yield reaches.

The DTG profiles are described below in more detail for each biomass material to observe the contrast in the experiments at same pressure but different temperatures and also compared with a biomass sample without treating (raw biomass).

Besides it will be represented a new plot method that could be useful for identify the global differences on the DTG peaks. This method has been called 'displacement', since the purpose of the plot is to show how displaced is the DTG profile for each experiment compared with the original profile for the raw material.

The displacement has been calculated with the global sum of all absolute value of the differences between the original DTG profile and the experimental DTG profile obtained. The plot will show the trend these displacements follows in function of the process temperature and pressure.

- Coffee
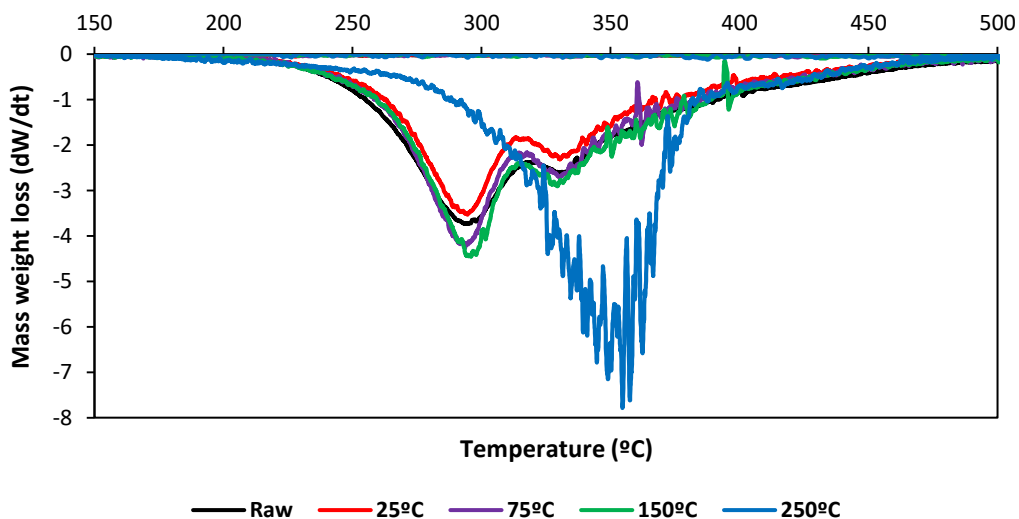
Fig. 11. DTG profiles for coffee at 1 bar.

22
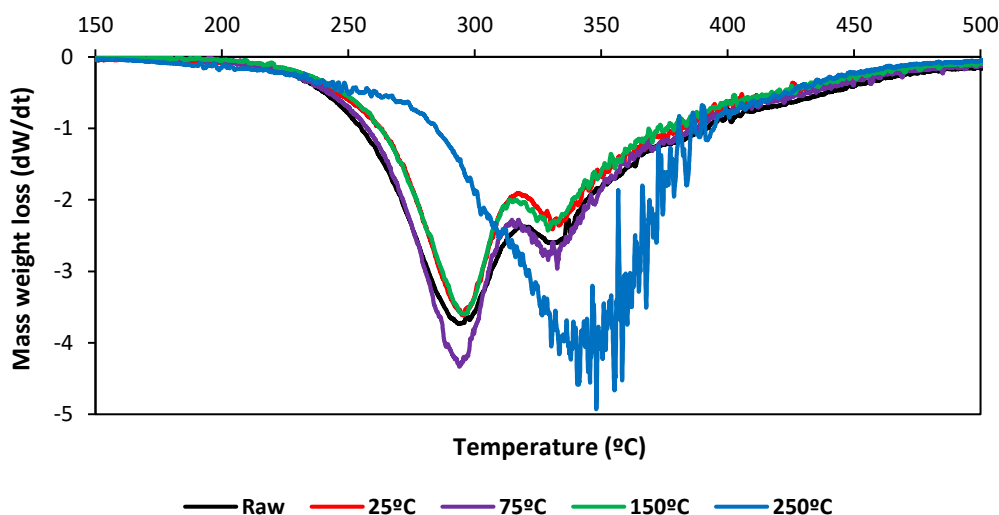
Fig. 12. DTG profiles for coffee at 50 bar.
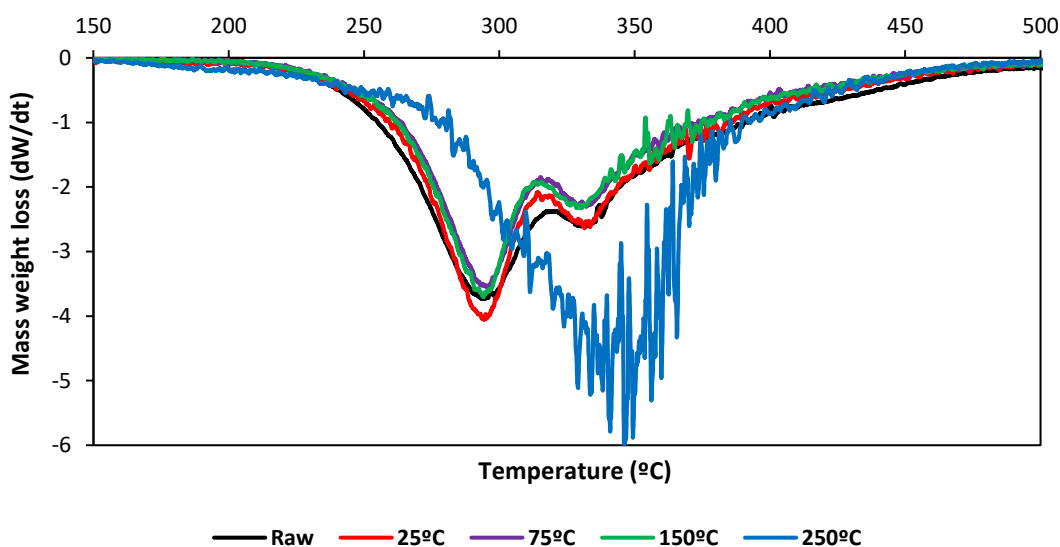
Fig. 13. DTG profiles for coffee at 240 bar.

In view of the results represented in Fig. 11, 12 and 13, despite of the noise in the signal of the experiments at 250ºC, it is remarkable the big difference between the profile of the experiments at the highest temperature and the rest of the experiments. This difference is equivalent to a change on the volatile composition since the shape of the profile is displaced to the right.

According to literature, the hemicellulose decomposition is observed at low temperatures, between 160-360ºC, whereas the volatilization of cellulose occurs at higher temperatures, typically between 240-400ºC. Unlike hemicellulose and cellulose, lignin is a molecule more complex and therefore, it has a wider range of decomposition temperatures,

noticeable at 200-700ºC (Ninduangdee et al., 2015). Thus, the first peak in the TGA profile is most probably hemicellulose and the second peak may be cellulose or lignin.
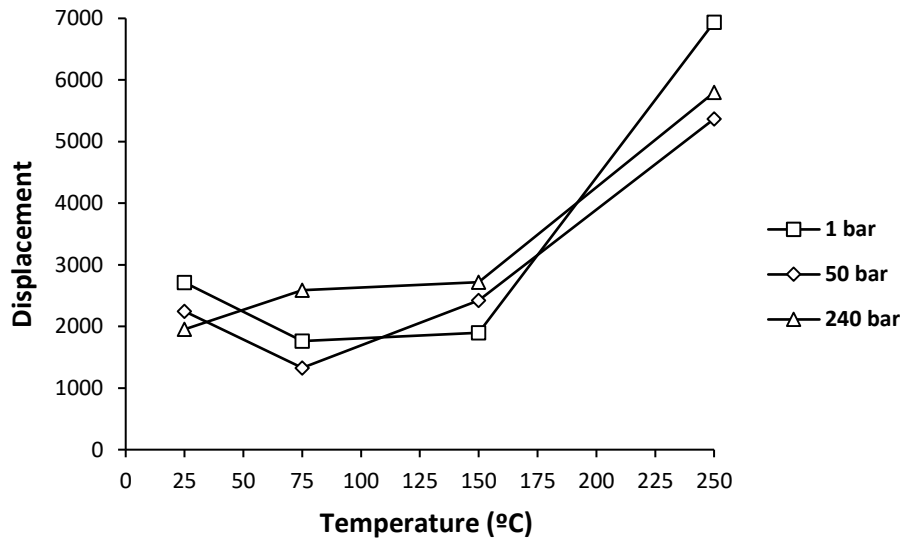
Fig. 14. Displacements for coffee at different temperatures and pressures.

Needless to say, the differences for coffee trials were quite clear in the DTG profiles, as the peak for the experiments that were performed at the highest temperature shows an abrupt shape with only one peak quite displaced to the right. Same behaviour is perceptible in Fig. 14 being the experiment at high temperature the ones that reach greater displacements.

▪ White wood
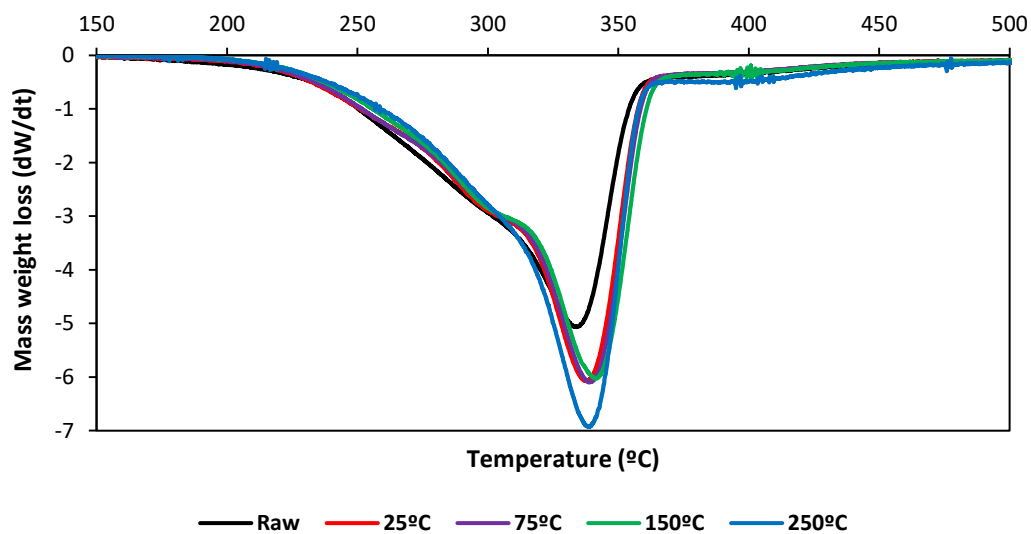
Fig. 15. DTG profiles for white wood at 1 bar.

24
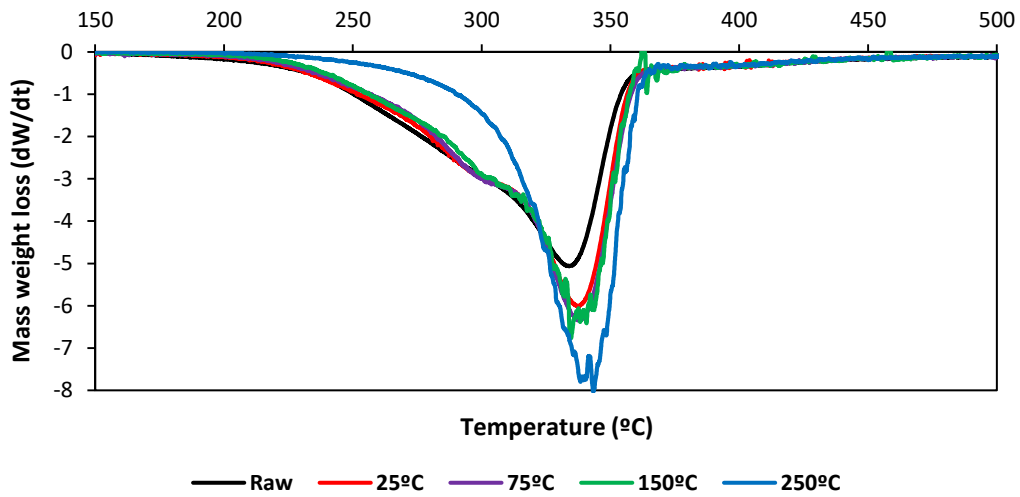
Fig. 16. DTG profiles for white wood at 50 bar.
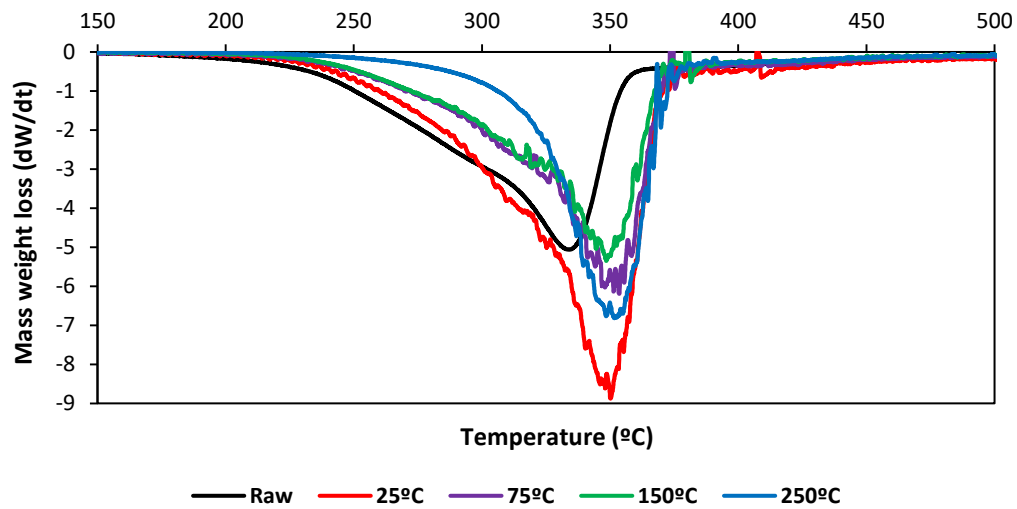
Fig. 17. DTG profiles for white wood at 240 bar.
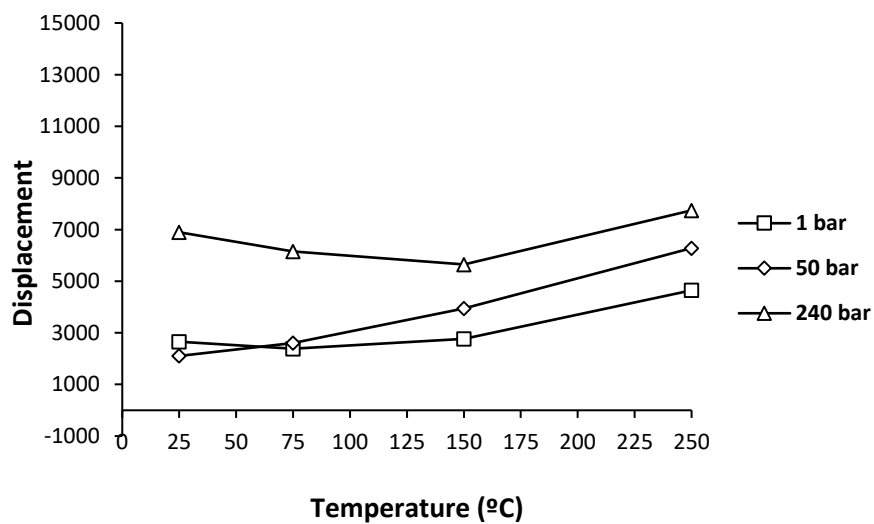
Fig. 18. Displacements for white wood at different temperatures and pressures.

In view of the white wood results it is worth mentioning the great displacements on the experiments at 50 bar at high temperatures in Fig. 16, in comparison with the rest of the experiments as seen in Fig. 18.

The peaks at the highest temperatures in liquid phase are the most successful because at this temperature it managed to break the hemicellulose peak remaining only one peak with longer shape that may be cellulose or lignin. Steam seems to be less effective with wood than with coffee.

- Rice
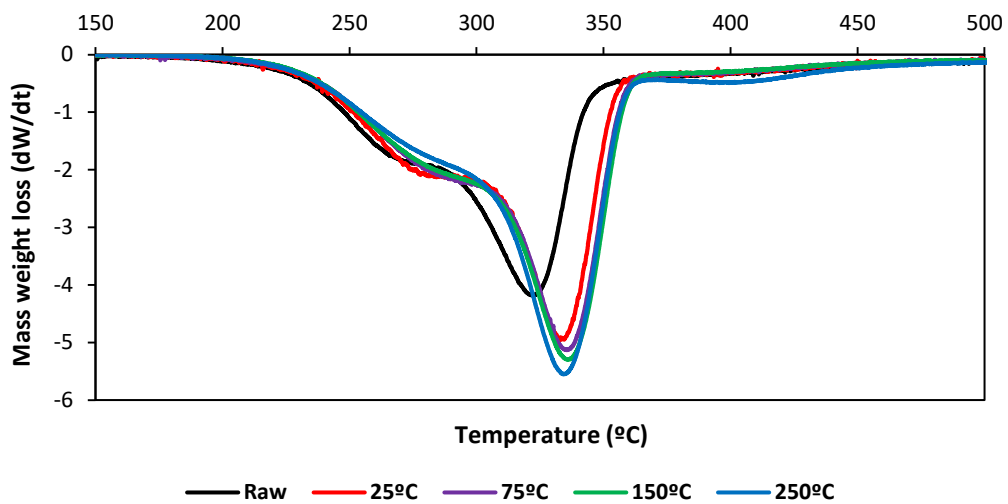
Fig. 19. DTG profiles for rice at 1 bar.
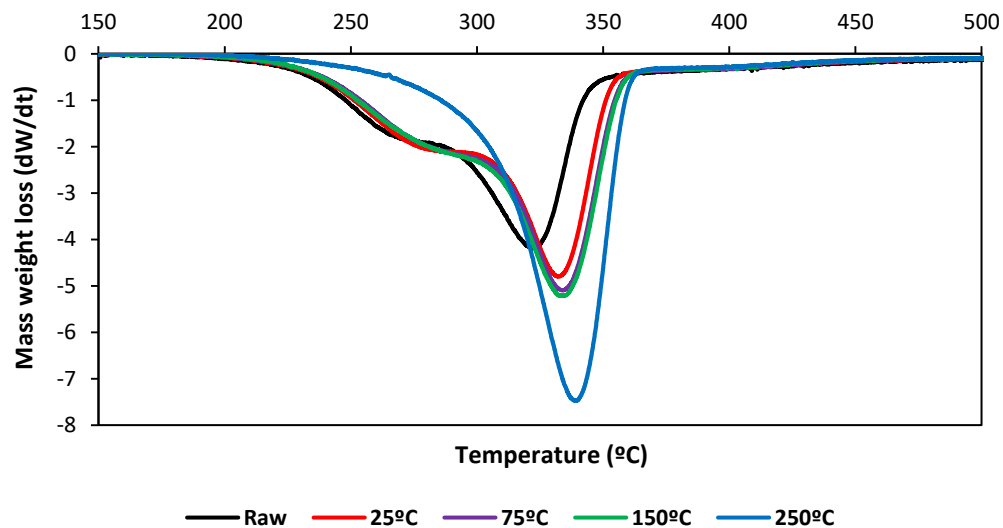
Fig. 20. DTG profiles for rice at 50 bar.
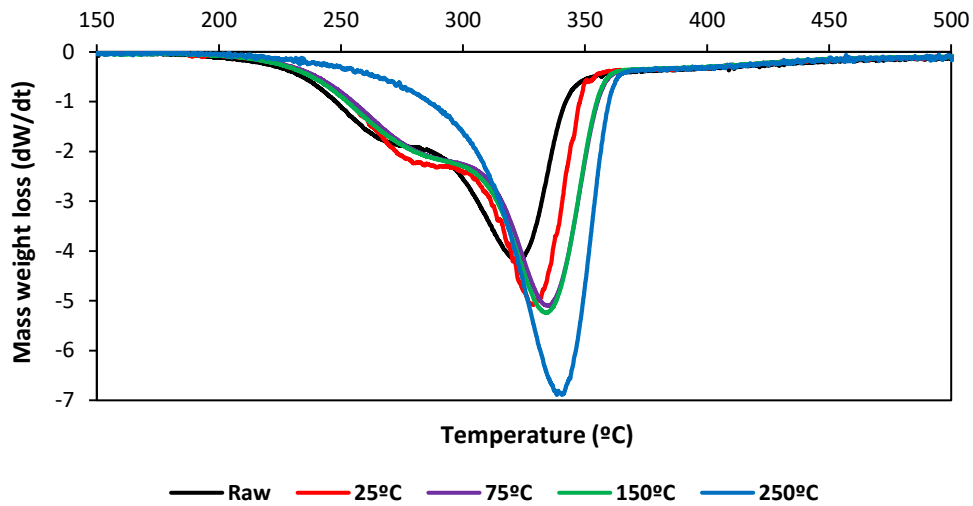
Fig. 21. DTG profiles for rice at 240 bar.
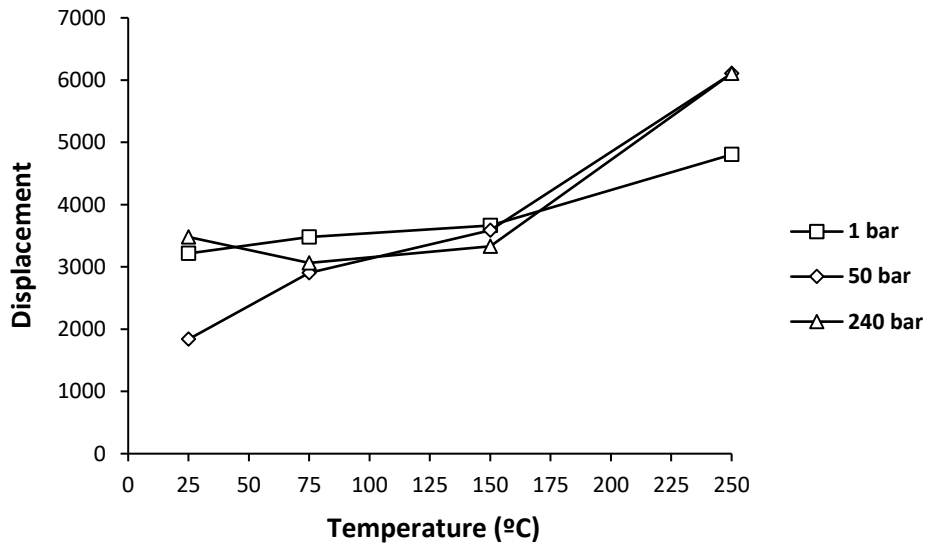
Fig. 22. Displacements for rice at different temperatures and pressures.

In view of the rice results, it should be noted that it follows similar behaviour as the white wood DTG profiles since the shape of the peaks at 250ºC (Fig. 20 and 21) are the longest achieving also the hemicellulose rupture. In addition, the displacements for the trials with steam achieved again smaller displacements.

- Lignin
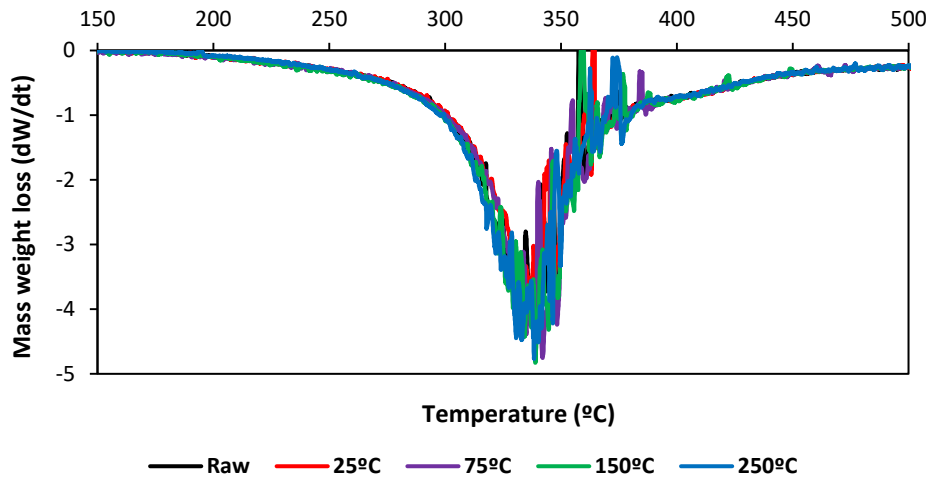
Fig. 23. DTG profiles for lignin at 1 bar.
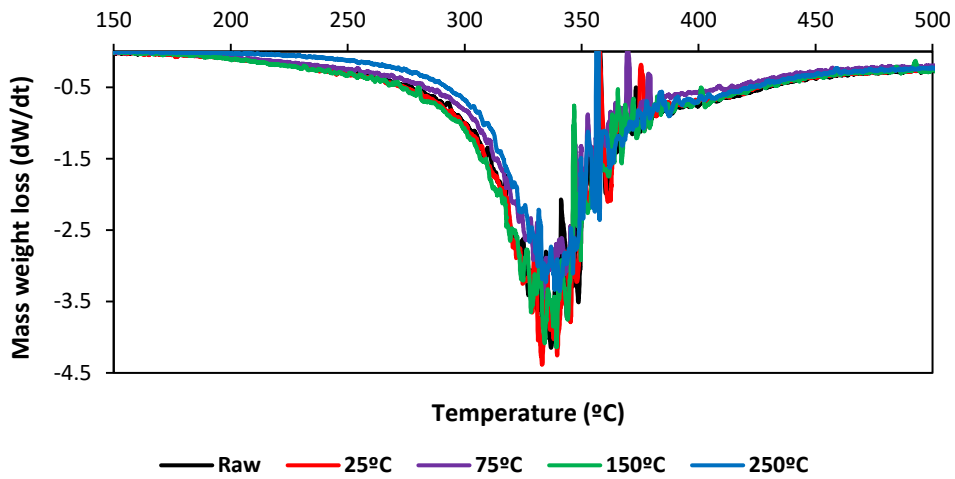
Fig. 24. DTG profiles for lignin at 50 bar.
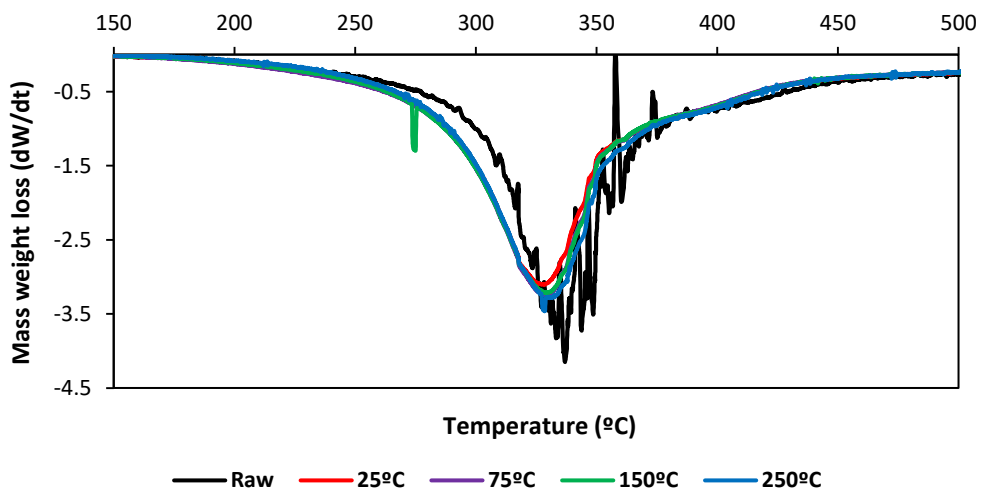
Fig. 25. DTG profiles for lignin at 240 bar.
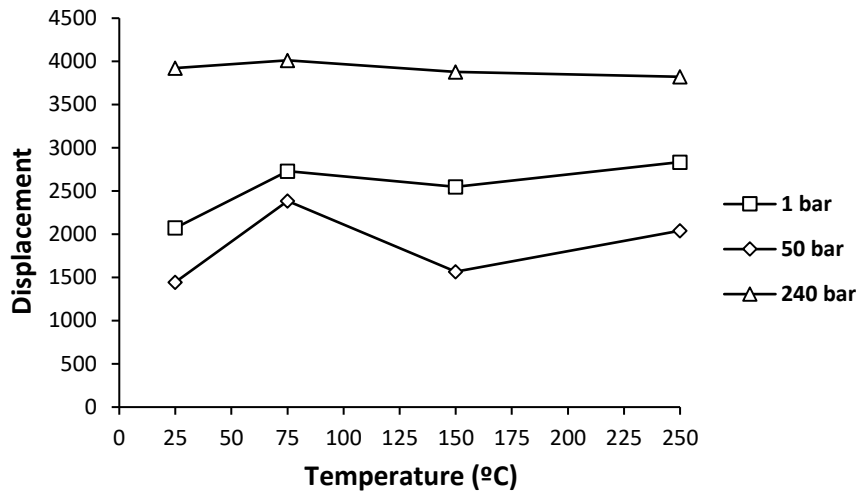
Fig. 26. Displacements for lignin at different temperatures and pressures.

The results obtained for lignin were quite different than the other biomasses. It can be seen in Fig. 23, 24 and 25 that the lignin profiles have a lot of noise in the signal. In any case, it can be appreciated in Fig. 26 that there is not a great change in any of the samples, since all of them achieved low and very similar displacements.

This behaviour might change if higher temperatures were used in the experiments due to lignin molecule need more energy to be affected.

- ▪ Zilkha
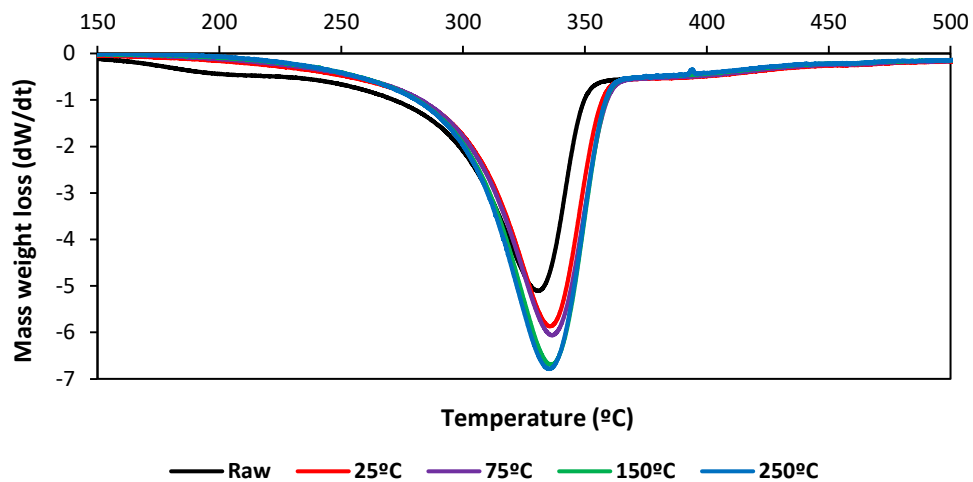
Fig. 27. DTG profiles for Zilkha at 1 bar.
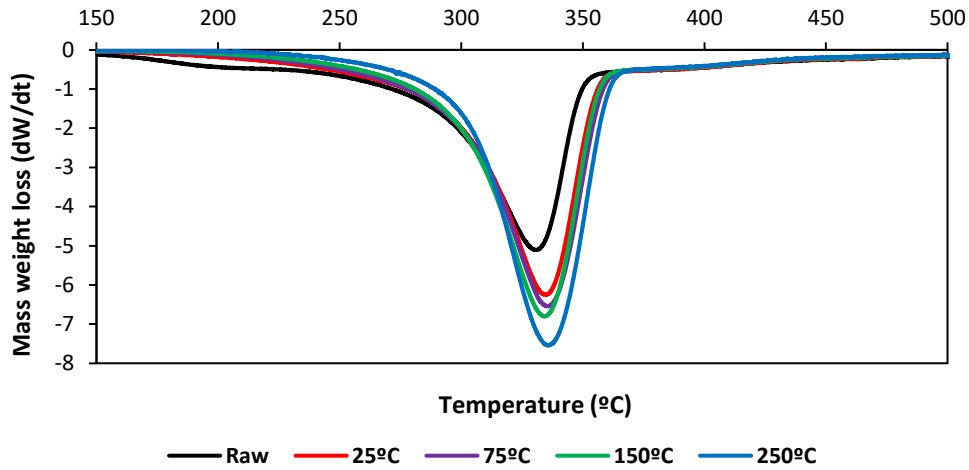
Fig. 28. DTG profiles for Zilkha at 50 bar.
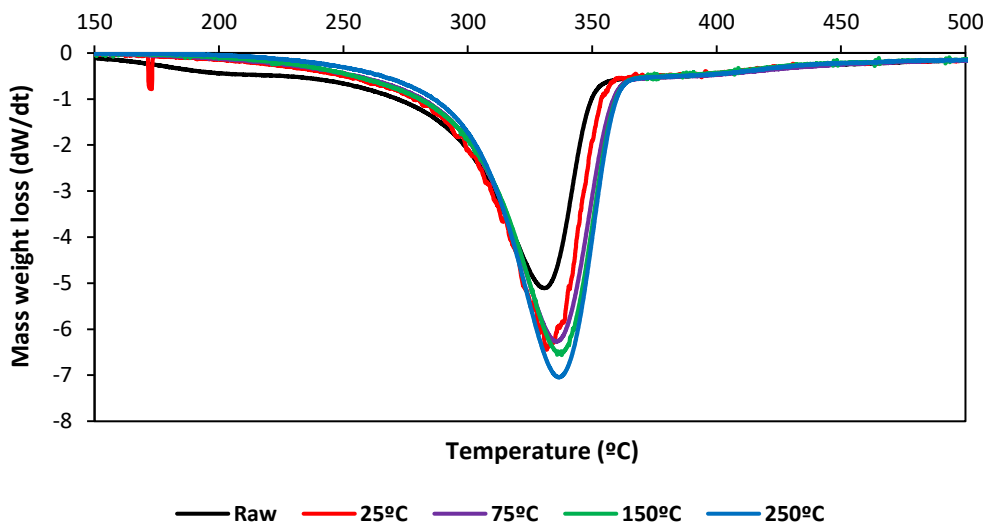
Fig. 29. DTG profiles for Zilkha at 240 bar.
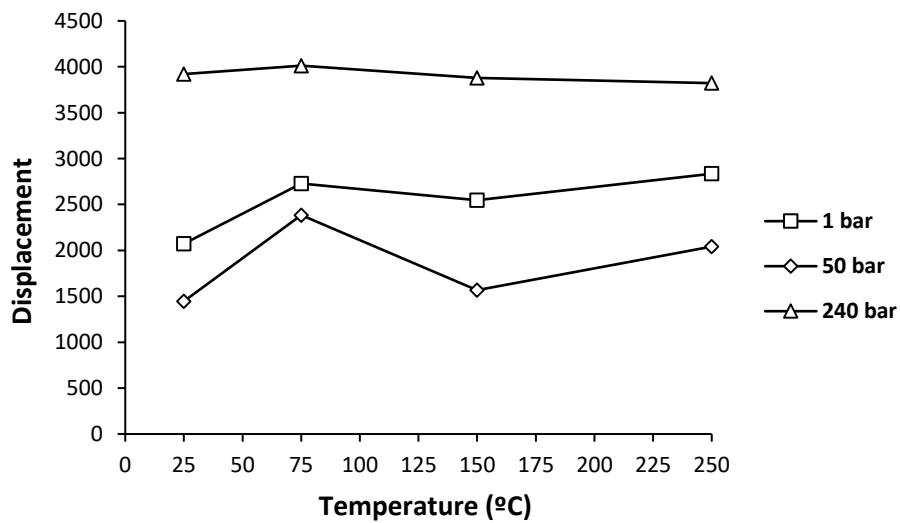
Fig. 30. Displacements for Zilkha at different temperatures and pressures.

The Zilkha results are similar to lignin. In this case, the DTG profiles in Fig 27, 28 and 29 have a little displacement to the right and also the peaks are longer for all experiments compared with the peak for raw Zilkha. As it can be seen in Fig. 30, there is not big changes in the displacements at different temperatures, being the trials at 250ºC narrowly the most displaced.

4.2.3. HPLC

The data collected for HPLC is showed below for each biomass feedstock. This data will give information about the number of components in the liquid sample and the concentration of these components.

- Coffee
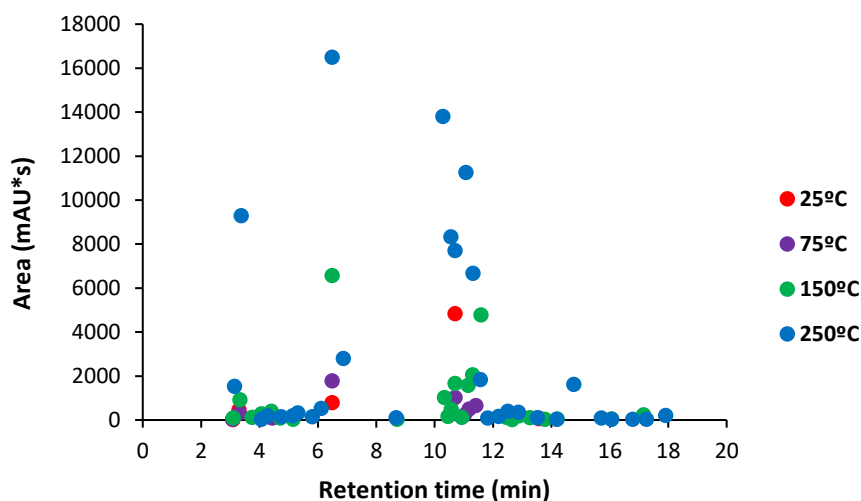
Fig. 31. Molecules found in HPLC for coffee at 1 bar.
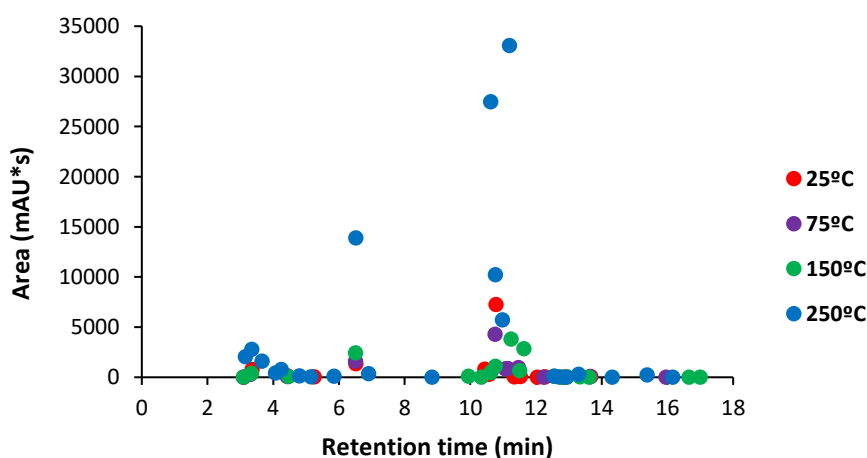
Fig. 32. Molecules found in HPLC for coffee at 50 bar.
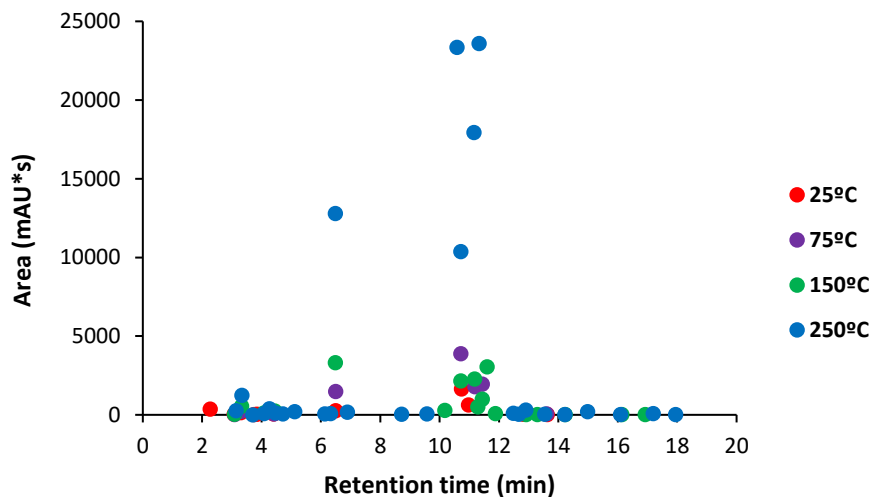
Fig. 33. Molecules found in HPLC for coffee at 240 bar.

The HPLC data for spent coffee shows a global distribution of retention times between 2 and 18 minutes. As it can be seen in Fig. 31, the experiment at 250ºC and 1 bar (steam as solvent) achieved the highest number of compounds while the molecules found at 50 bar and 240 bar (Fig. 32 and 33) obtained less number of molecules but more concentrated. It was expected that HPLC results were also related with the yields achieved.

- White wood
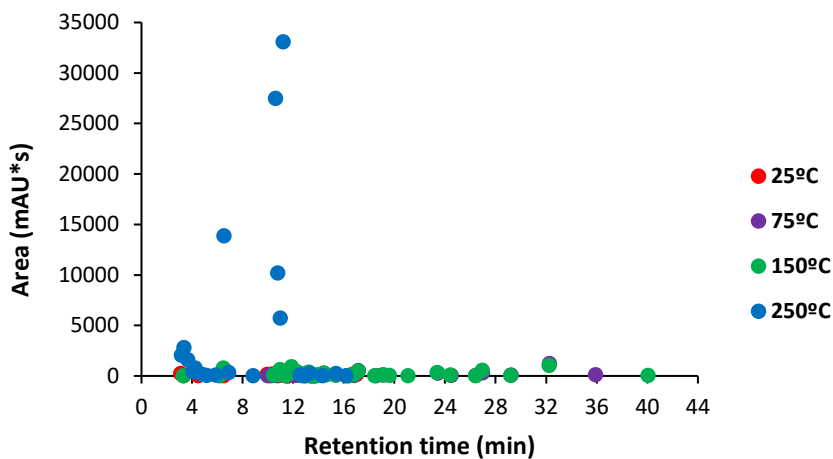
Fig. 34. Molecules found in HPLC for white wood at 1 bar.
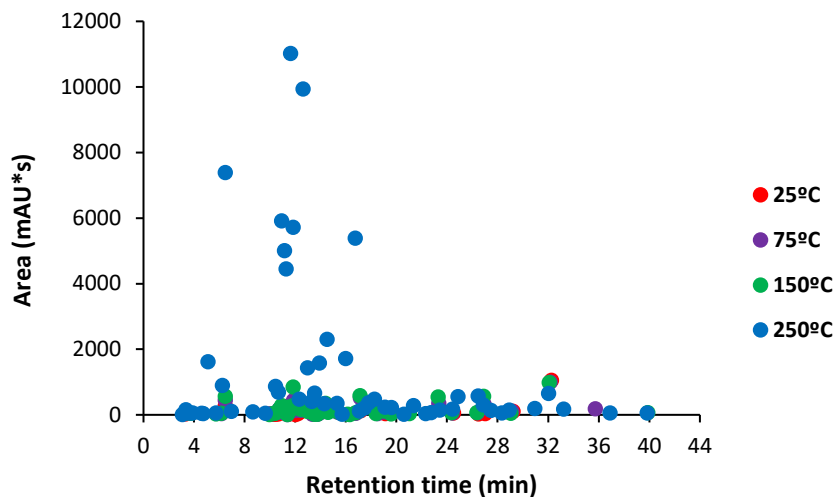
Fig. 35. Molecules found in HPLC for white wood at 50 bar.
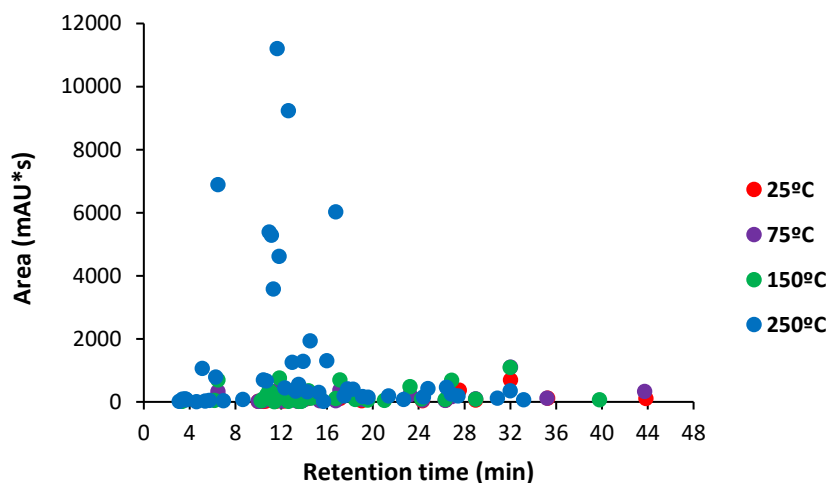
Fig. 36. Molecules found in HPLC for white wood at 240 bar.

The HPLC results in Fig 34, 35 and 36 show that white wood liquid samples had greater number of compounds distributed between 3 and 44 minutes of retention time.

Unlike the coffee trials, higher number of molecules were found for experiments at 50 and 240 bar and, on the contrary, the most concentrated compounds were achieved with steam at 1 bar and 250ºC.
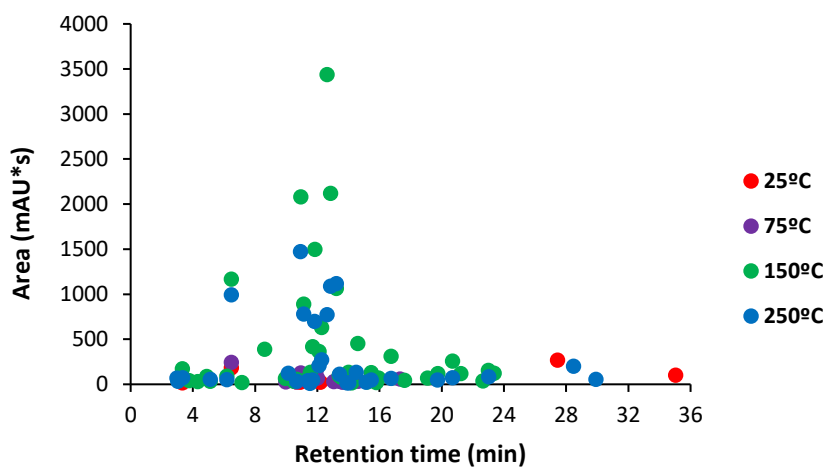
- Rice

Fig. 37. Molecules found in HPLC for rice at 1 bar.
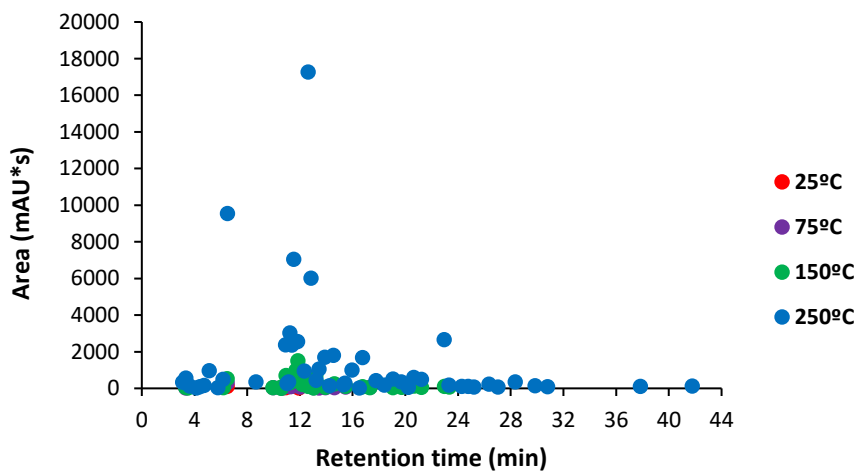
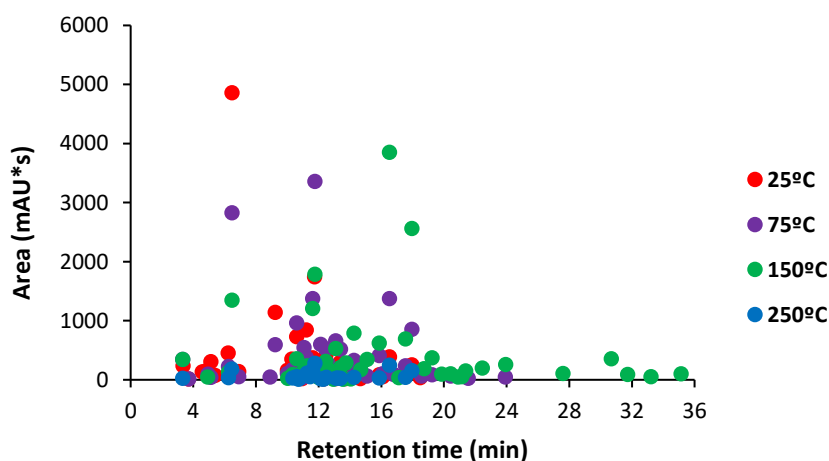**Fig. 38.** Molecules found in HPLC for rice at 50 bar.
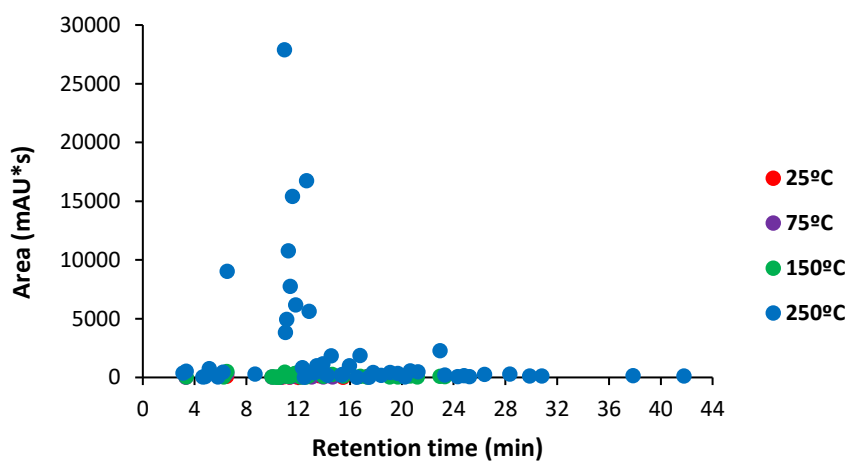
Fig. 39. Molecules found in HPLC for rice at 240 bar.

Following similar behaviour than wood results, steam did not work well with rice in since experiments at lower temperatures achieved more concentrated compounds (Fig. 37). The largest number of compounds was obtained at 250ºC and 50 bar as seen in Fig. 38. Retention times for rice were between 3 and 28 minutes.

- Lignin
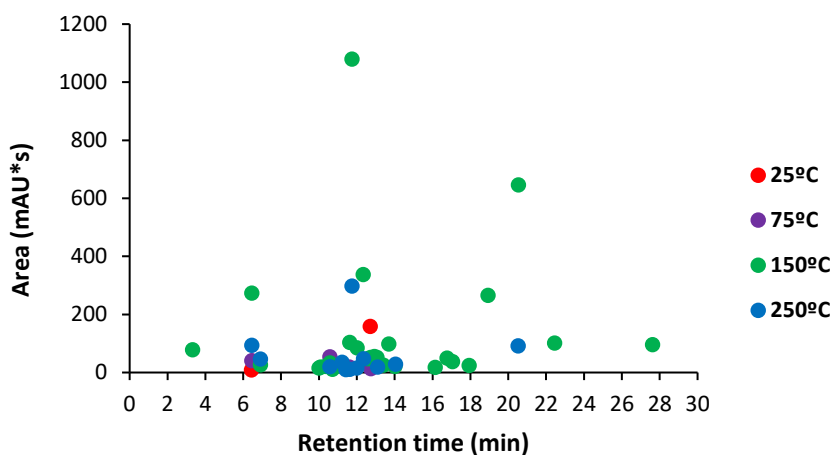
Fig. 40. Molecules found in HPLC for lignin at 1 bar.
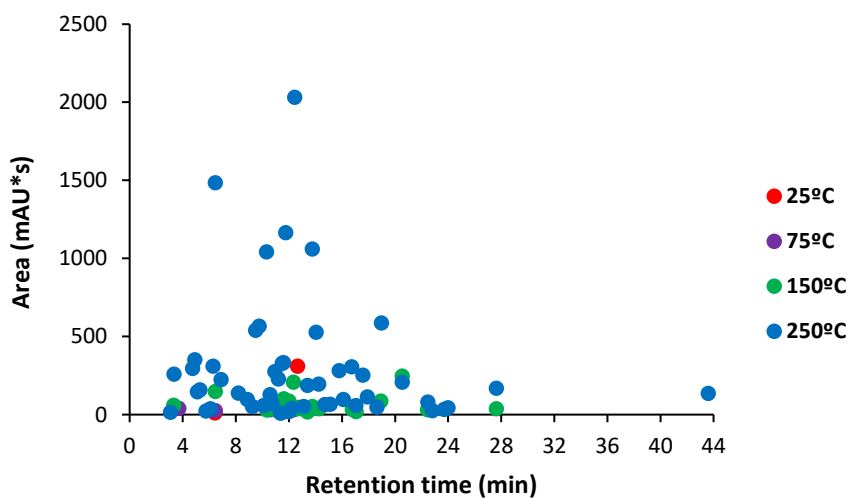
Fig. 41. Molecules found in HPLC for lignin at 50 bar.
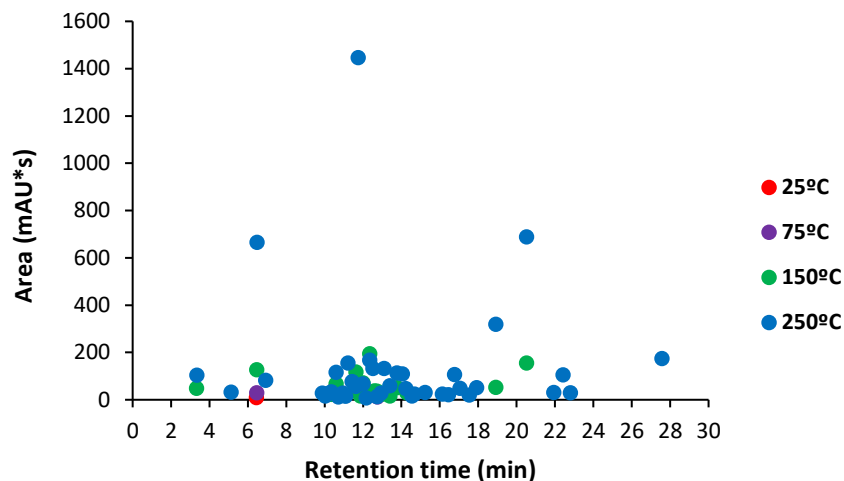
Fig. 42. Molecules found in HPLC for lignin at 240 bar.

HPLC results for lignin show quite low concentrations in comparison with the rest of biomass feedstocks, which is logical since lignin yields were the lowest. Lower compounds and concentrations were obtained with steam (Fig. 40) compared with the results at 150ºC with water in liquid phase. Retention times for lignin were between 2 and 28 minutes.

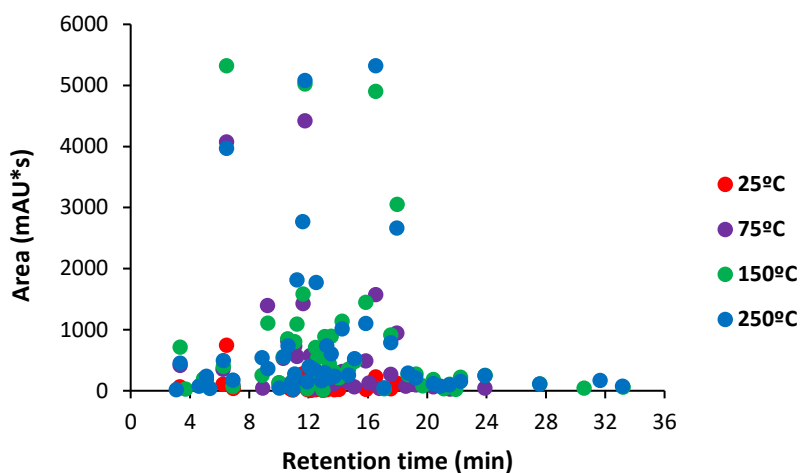- Zilkha

Fig. 43. Molecules found in HPLC for Zilkha at 1 bar.

Fig. 44. Molecules found in HPLC for Zilkha at 50 bar.
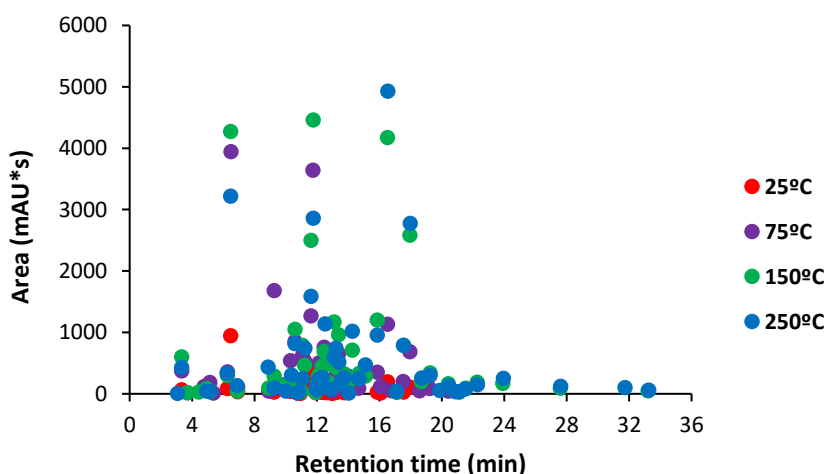
Fig. 45. Molecules found in HPLC for Zilkha at 240 bar.

The retention times for Zilkha samples were between 3 and 34 minutes. Similar to lignin results, steam does not affect Zilkha powder either. However, as Fig 44 and 45 show, a large number of compounds but with low concentrations were found at 50 and 240 bar working both at low and high temperatures

4.2.4. MALDI-TOF-MS

The characterization with MALDI is more abstract and complicated than the rest of analyse methods due to the high capacity of the equipment, which can easily be affected by external noise or even by the matrix used with the sample.

The MALDI desorption laser give two spectrum data, one for the positive ions and other for the negative ions. It has been chosen to represent the most relevant in each case.
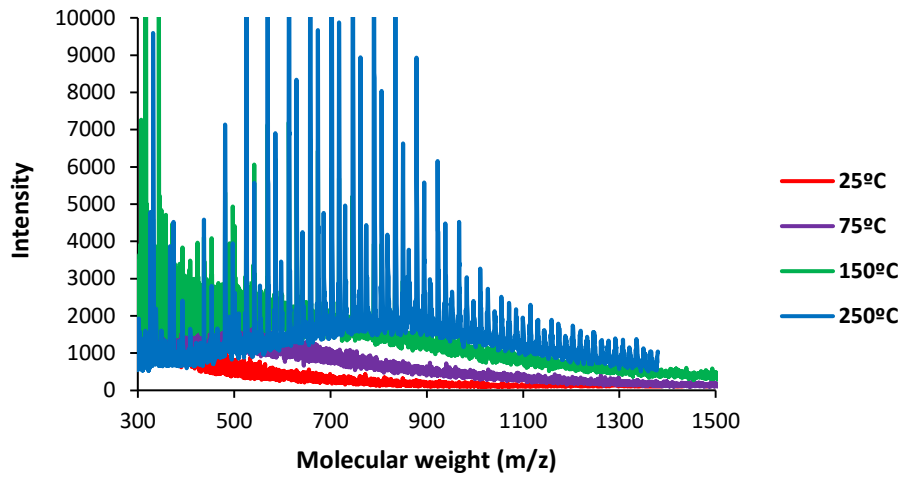
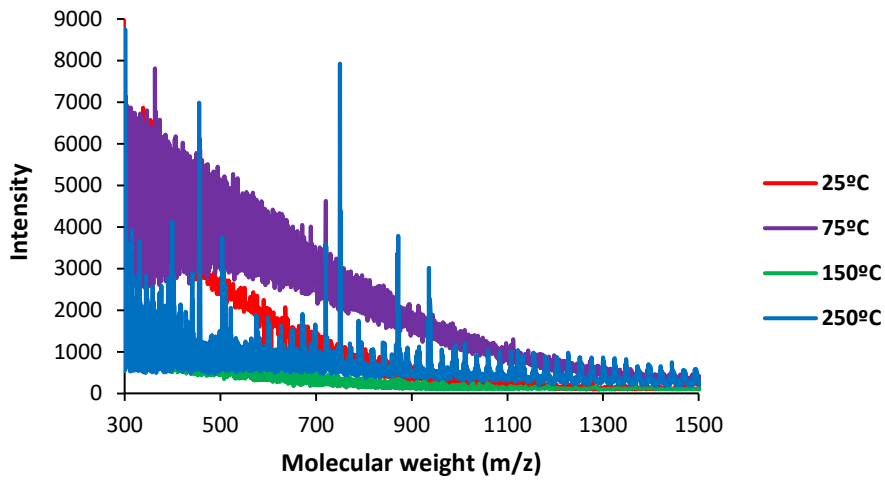■ Coffee

Fig. 46. MALDI-TOF spectrum of coffee at 1 bar.

Fig. 47. MALDI-TOF spectrum of coffee at 50 bar.
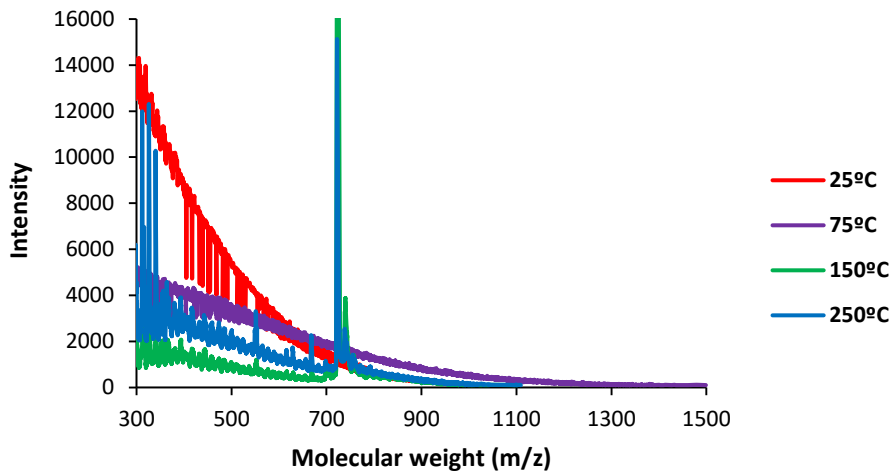

Fig. 48. MALDI-TOF spectrum of coffee at 240 bar.

Once the coffee samples were dried a brown solid remained in the sample pot. The coffee was the biomass feedstock that produced the highest amount of dried solids.

The spectrums in Fig 46, 47 and 48 shows a molecular weight distribution more shifted to the right, for the experiments at the highest temperature (250°C) in comparison with the rest of the temperatures, which means that bigger molecules were achieved. Decreasing the pressure, the shift is more evident.
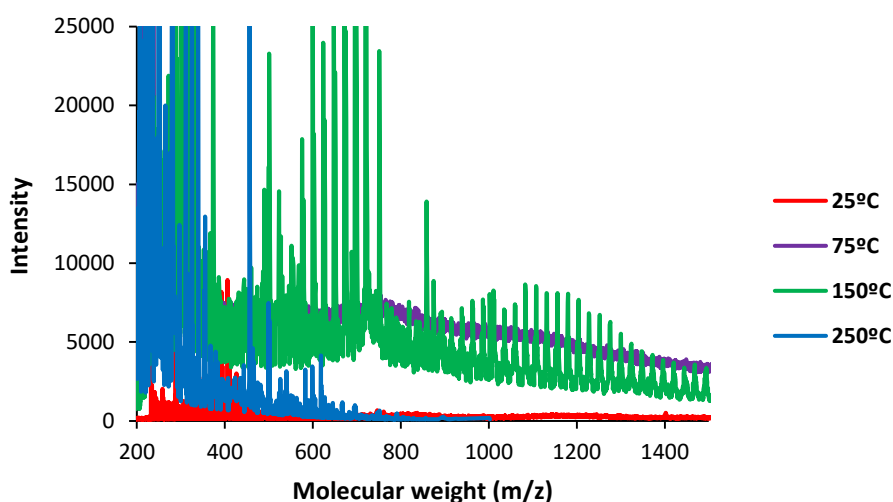
- White wood

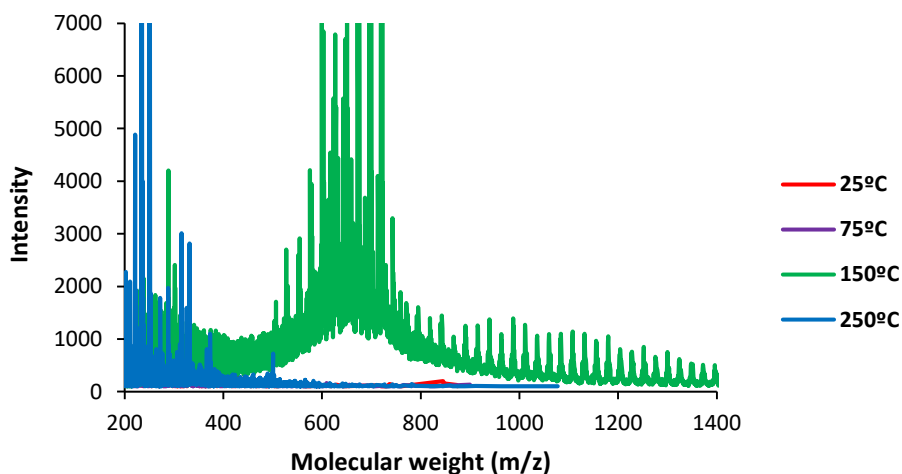**Fig. 49.** MALDI-TOF spectrum of white wood at 1 bar.

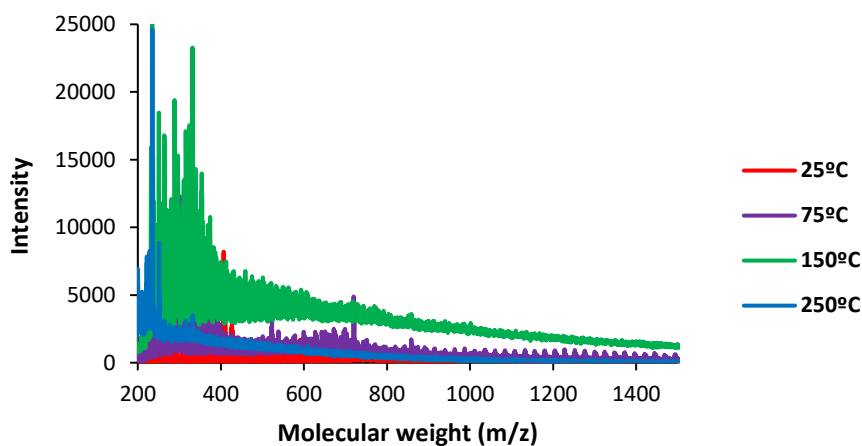**Fig. 50.** MALDI-TOF spectrum of white wood at 50 bar.

Fig. 51. MALDI-TOF spectrum of white wood at 240 bar.

The white wood spectrum shows different behaviour than coffee spectrum. The most displaced spectrum was achieved at 150ºC as seen in Fig 49, 50 and 51. Higher concentrations but smaller molecules were obtained for experiment with steam at 1 bar and 250ºC (Fig. 49).
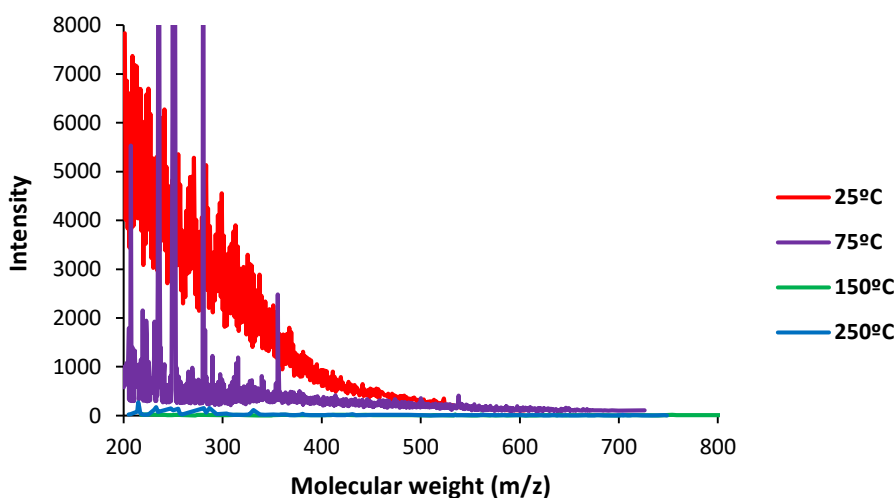
- Rice

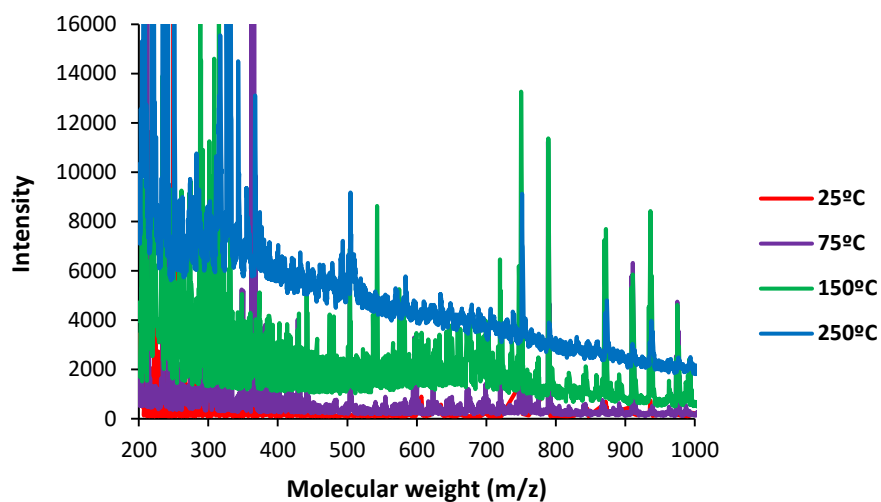**Fig. 52.** MALDI-TOF spectrum of rice at 1 bar.

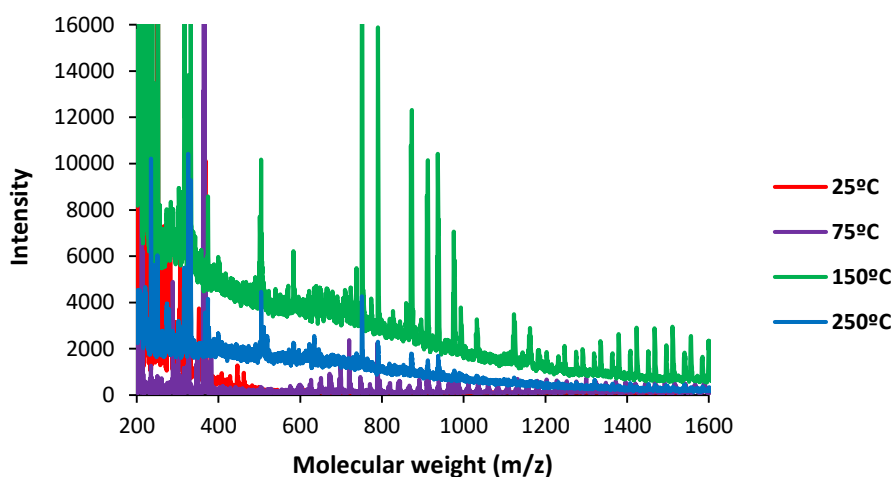**Fig. 53.** MALDI-TOF spectrum of rice at 50 bar.

Fig. 54. MALDI-TOF spectrum of rice at 240 bar.

As appreciated in Fig. 52, rice spectrums at 1 bar and 150ºC and 250ºC had quite low intensities compared with the spectrums at lower temperature. Opposite behaviour happened when working at medium and high pressure in Fig 53 and 54 respectively, which molecular distributions marked a decreasing trend showing greater predominance for compounds with low molecular weight.
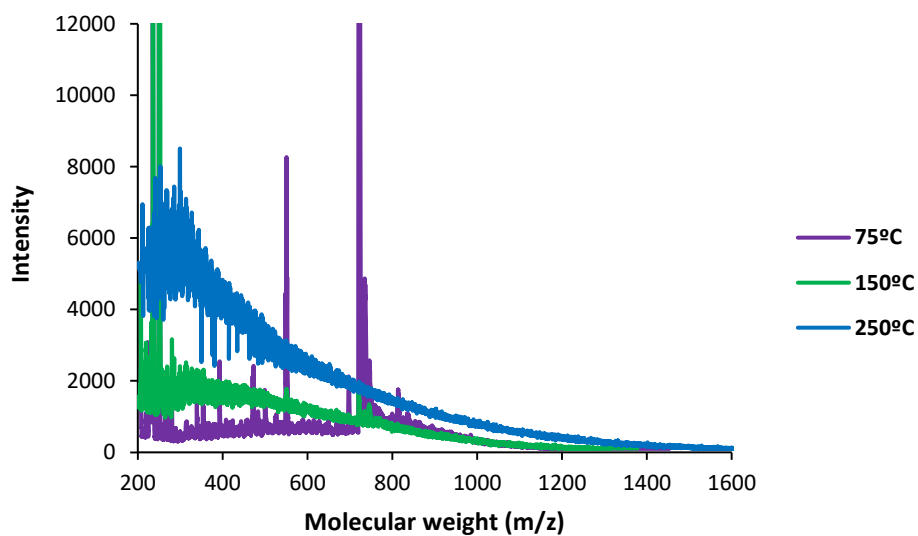
- Lignin

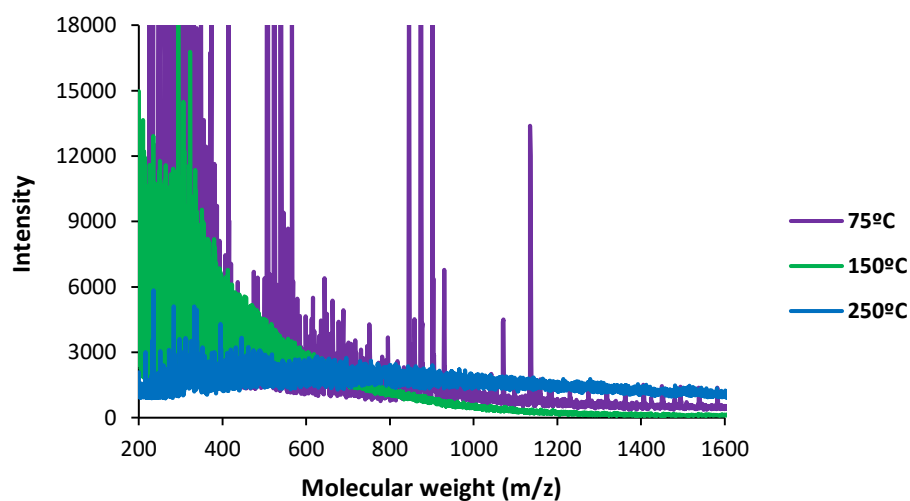**Fig. 55.** MALDI-TOF spectrum of lignin at 1 bar.

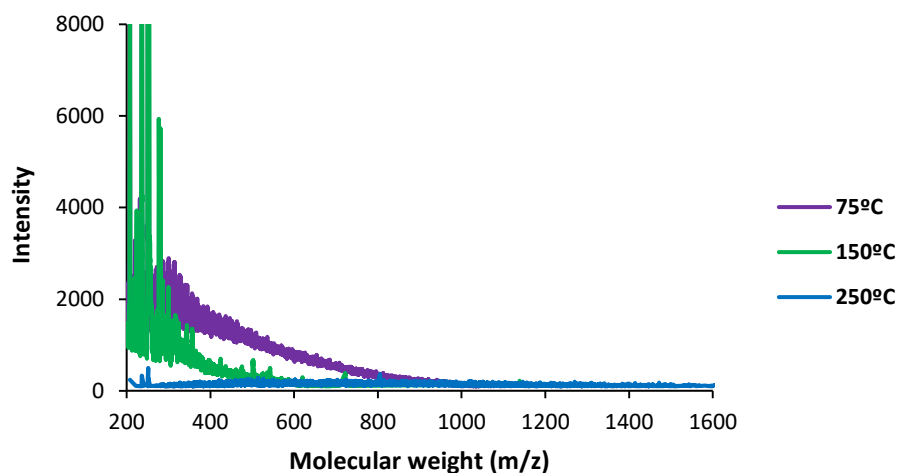**Fig. 56.** MALDI-TOF spectrum of lignin at 50 bar.

Fig. 57. MALDI-TOF spectrum of lignin at 240 bar.

It should be noted that the samples obtained at 25ºC for lignin were completely empty after letting them dry so they could not be analysed by MALDI technique. Fig. 55 shows predominance of low molecular weight compounds while working at 1 bar, being the experiment at 250ºC the analyse with the most intense spectrum. However, quite different spectrums were obtained in Fig 56 and 57 since lower temperatures achieved higher concentrations of low molecular weight compounds while at 250ºC the spectrum obtained showed almost the same intensity for all the range.

- Zilkha
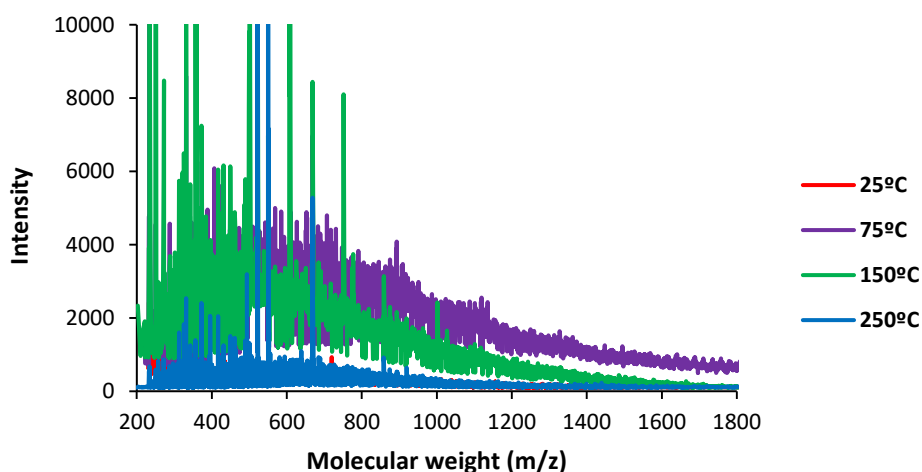
Fig. 58. MALDI-TOF spectrum of Zilkha at 1 bar.
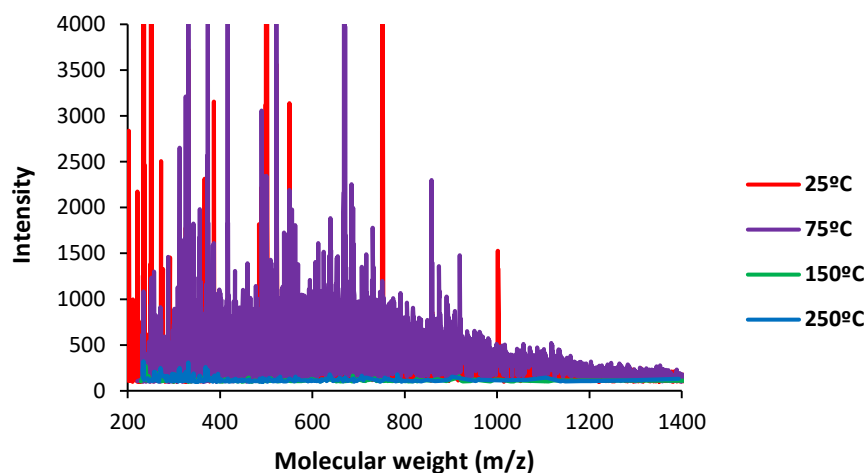
Fig. 59. MALDI-TOF spectrum of Zilkha at 50 bar.
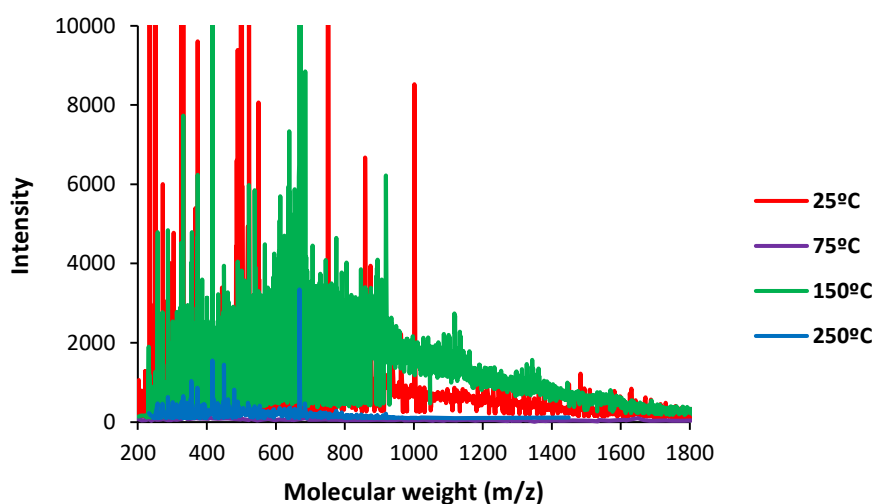
Fig. 60. MALDI-TOF spectrum of Zilkha at 240 bar.

It is worth noting that for Zilkha all the spectrums at 250ºC obtained very low intensities, which may be a technical error the MALDI equipment gave since the sample was very concentrated. For the rest of temperatures, at low pressures the spectrum at 75ºC achieved higher concentrations for the whole molecular weight range (Fig. 58 and 59) while at the highest pressure the spectrum at 150ºC was the most predominant (Fig. 60).

5. Conclusions

In this study, the characterization of both liquid and solid products obtained from the hydrothermal carbonization of 5 different types of biomass feedstock was investigated.

The reaction conditions were carefully managed by a digital temperature controller and a back-pressure regulator. By varying these conditions, the results obtained in the different characterization methods were discussed.

The highest char yields were achieved from spent coffee, reaching values up to almost 70% when reacted with steam at high temperature. On the contrary, lignin proved to be the most resistant material to the carbonization, not surpassing yields higher than 13% even at the most extreme reaction conditions.

Some similarities between the yields and the thermogravimetric curves obtained afterwards were found. The devolatilization temperature of coffee, was the lowest of all the biomasses and, as expected, the devolatilization temperature of lignin was the highest.

From a new proposed method called 'displacement', it was easier to identify the differences between the thermogravimetric behaviour of untreated biomass and the remaining solid biomass after the reaction. These differences were more evident with changes in temperature than by changing the pressure. Higher displacements were observed as a function of temperature working with spent coffee and white wood than when working with lignin, which barely achieved significant displacements.

By means of liquid chromatography (HPLC), it was possible to obtain a relation between the concentrations and the number of components analysed in the liquid product sample as a function of the reaction conditions. All raw materials obtained higher concentrations when reacted with superheated liquid water than when they reacted with steam except spent coffee. Lignin was the material that released less components to the liquid phase.

Finally, by using MALDI-TOF-MS it was possible to obtain the spectrum of the remaining solid in the liquid sample after allowing it to dry. These spectrums showed certain relations in some feedstocks between the reaction temperature and the molecular weight distribution. Lignin samples carried out at 25ºC were totally empty after drying due to the low concentrations obtained.

Acknowledgements

References

Abdoulmoumine, N., Adhikari, S., Kulkarni, A., & Chattanathan, S. (2015). A review on biomass gasification syngas cleanup. *Applied Energy*, *155*, 294–307. https://doi.org/10.1016/j.apenergy.2015.05.095

Álvarez-Murillo, A., Sabio, E., Ledesma, B., Román, S., & González-García, C. M. (2016). Generation of biofuel from hydrothermal carbonization of cellulose. Kinetics modelling. *Energy*, *94*, 600–608. https://doi.org/10.1016/j.energy.2015.11.024

Arellano, O., Flores, M., Guerra, J., Hidalgo, A., Rojas, D., & Strubinger, A. (2016). Hydrothermal carbonization of corncob and characterization of the obtained hydrochar. *Chemical Engineering Transactions*, *50*, 235–240. https://doi.org/10.3303/CET1650040

Berge, N. D., Ro, K. S., Mao, J., Flora, J. R. V, Chappell, M. A., & Bae, S. (2011). Hydrothermal Carbonization of Municipal Waste Streams. *Environmental Science & Technology*, *45*(13), 5696–5703. https://doi.org/10.1021/es2004528

Cheng, S., D'cruz, I., Wang, M., Leitch, M., & Xu, C. (Charles). (2010). Highly Efficient Liquefaction of Woody Biomass in Hot-Compressed Alcohol−Water Co-solvents. *Energy & Fuels*, *24*(9), 4659–4667. https://doi.org/10.1021/ef901218w

Cherad, R., Onwudili, J. A., Biller, P., Williams, P. T., & Ross, A. B. (2016). Hydrogen production from the catalytic supercritical water gasification of process water generated from hydrothermal liquefaction of microalgae. *Fuel*, *166*, 24–28. https://doi.org/10.1016/j.fuel.2015.10.088

Dimitriadis, A., & Bezergianni, S. (2017). Hydrothermal liquefaction of various biomass and waste feedstocks for biocrude production: A state of the art review. *Renewable and Sustainable Energy Reviews*, *68*, 113–125. https://doi.org/10.1016/j.rser.2016.09.120

Flexer, V., Donose, B. C., Lefebvre, C., Pozo, G., Boone, M. N., Van Hoorebeke, L., … Brun, N. (2016). Microcellular Electrode Material for Microbial Bioelectrochemical Systems Synthesized by Hydrothermal Carbonization of Biomass Derived Precursors. *ACS Sustainable Chemistry & Engineering*, *4*(5), 2508–2516. https://doi.org/10.1021/acssuschemeng.5b01592

Gollakota, A R K, Kishore, N., & Gu, S. (2018). A review on hydrothermal liquefaction of biomass. *Renewable and Sustainable Energy Reviews*, *81*, 1378–1392. https://doi.org/10.1016/j.rser.2017.05.178

Gollakota, Anjani R K, Reddy, M., Subramanyam, M. D., & Kishore, N. (2016). A review on the upgradation techniques of pyrolysis oil. *Renewable and Sustainable Energy Reviews*, *58*, 1543–1568. https://doi.org/10.1016/j.rser.2015.12.180

Güngören Madenoğlu, T., Sağlam, M., Yüksel, M., & Ballice, L. (2016). Hydrothermal gasification of biomass model compounds (cellulose and lignin alkali) and model mixtures. *The Journal of Supercritical Fluids*, *115*, 79–85. https://doi.org/10.1016/j.supflu.2016.04.017

Heidari, M., Dutta, A., Acharya, B., & Mahmud, S. (2018). A review of the current knowledge and challenges of hydrothermal carbonization for biomass conversion. *Journal of the Energy Institute*. https://doi.org/10.1016/j.joei.2018.12.003

Jensen, M. M., Djajadi, D. T., Torri, C., Rasmussen, H. B., Madsen, R. B., Venturini, E., … Glasius, M. (2018). Hydrothermal Liquefaction of Enzymatic Hydrolysis Lignin: Biomass Pretreatment Severity Affects Lignin Valorization. *ACS Sustainable Chemistry & Engineering*, *6*(5), 5940–5949. https://doi.org/10.1021/acssuschemeng.7b04338

Kim, J. G., Kim, J. H., Song, B.-J., Jeon, Y. P., Lee, C. W., Lee, Y.-S., & Im, J. S. (2016). Characterization of pitch derived from pyrolyzed fuel oil using TLC-FID and MALDI-TOF. *Fuel*, *167*, 25–30. https://doi.org/10.1016/j.fuel.2015.11.050

Köchermann, J., Görsch, K., Wirth, B., Mühlenberg, J., & Klemm, M. (2018). Hydrothermal carbonization: Temperature influence on hydrochar and aqueous phase composition during process water recirculation. *Journal of Environmental Chemical Engineering*, *6*(4), 5481–5487. https://doi.org/10.1016/j.jece.2018.07.053

Kruse, A., Funke, A., & Titirici, M.-M. (2013). Hydrothermal conversion of biomass to fuels and energetic materials. *Current Opinion in Chemical Biology*, *17*(3), 515–521. https://doi.org/10.1016/j.cbpa.2013.05.004

Kumar, M., Olajire Oyedun, A., & Kumar, A. (2018). A review on the current status of various hydrothermal technologies on biomass feedstock. *Renewable and Sustainable Energy Reviews*, *81*, 1742–1770. https://doi.org/10.1016/j.rser.2017.05.270

Lester, E., Avila, C., Pang, C. H., Williams, O., Perkins, J., Gaddipatti, S., … Wu, T. (2018). A proposed biomass char classification system. *Fuel*, *232*, 845–854. https://doi.org/10.1016/j.fuel.2018.05.153

Lester, E., Gong, M., & Thompson, A. (2007). A method for source apportionment in biomass/coal blends using thermogravimetric analysis. *Journal of Analytical and Applied Pyrolysis*, *80*(1), 111–117. https://doi.org/10.1016/j.jaap.2007.01.010

Li, H., Liu, Z., Zhang, Y., Li, B., Lu, H., Duan, N., … Si, B. (2014). Conversion efficiency and oil quality of low-lipid high-protein and high-lipid low-protein microalgae via hydrothermal liquefaction. *Bioresource Technology*, *154*, 322–329. https://doi.org/10.1016/j.biortech.2013.12.074

Ninduangdee, P., Kuprianov, V. I., Cha, E. Y., Kaewrath, R., Youngyuen, P., & Atthawethworawuth, W. (2015). Thermogravimetric Studies of Oil Palm Empty Fruit Bunch and Palm Kernel Shell: TG/DTG Analysis and Modeling. *Energy Procedia*, *79*, 453–458. https://doi.org/10.1016/j.egypro.2015.11.518

Pedersen, T. H., Grigoras, I. F., Hoffmann, J., Toor, S. S., Daraban, I. M., Jensen, C. U., … Rosendahl, L. A. (2016). Continuous hydrothermal co-liquefaction of aspen wood and glycerol with water phase recirculation. *Applied Energy*, *162*, 1034–1041. https://doi.org/10.1016/j.apenergy.2015.10.165

Perlt, E., von Domaros, M., Kirchner, B., Ludwig, R., & Weinhold, F. (2017). Predicting the Ionic Product of Water. *Scientific Reports*, *7*(1), 10244. https://doi.org/10.1038/s41598-017-10156-w

Peterson, A. A., Vogel, F., Lachance, R. P., Fröling, M., Antal Michael J., J., & Tester, J. W. (2008). Thermochemical biofuel production in hydrothermal media: A review of sub- and supercritical water technologies. *Energy & Environmental Science*, *1*(1), 32–65. https://doi.org/10.1039/B810100K

Pińkowska, H., & Oliveros, E. (2014). Application of the Doehlert Matrix for the Determination of the Optimal Conditions of Hydrolysis of Soybean Protein in Subcritical Water. *Industrial & Engineering Chemistry Research*, *53*(4), 1320–1326. https://doi.org/10.1021/ie403451b

Sajjadi, B., Chen, W.-Y., Raman, A. A. A., & Ibrahim, S. (2018). Microalgae lipid and biomass for biofuel production: A comprehensive review on lipid enhancement strategies and their effects on fatty acid composition. *Renewable and Sustainable Energy Reviews*, *97*, 200–232. https://doi.org/10.1016/j.rser.2018.07.050

Santos, I. C., Hildenbrand, Z. L., & Schug, K. A. (2016). Applications of MALDI-TOF MS in environmental microbiology. *Analyst*, *141*(10), 2827–2837. https://doi.org/10.1039/C6AN00131A

Savage, P. E., Levine, R. B., & Huelsman, C. M. (2010). Hydrothermal processing of biomass. *RSC Energy and Environment Series*, Vol. 2010, pp. 192–221. Retrieved from https://www.scopus.com/inward/record.uri?eid=2-s2.0-84878390446&partnerID=40&md5=2126608e89536729b219082ab825fa5c

Shi, W., Li, S., Jia, J., & Zhao, Y. (2013). Highly Efficient Conversion of Cellulose to Bio-Oil in Hot-Compressed Water with Ultrasonic Pretreatment. *Industrial & Engineering Chemistry Research*, *52*(2), 586–593. https://doi.org/10.1021/ie3024966

Singh, R., Bhaskar, T., & Balagurumurthy, B. (2015). Effect of solvent on the hydrothermal liquefaction of macro algae Ulva fasciata. *Process Safety and Environmental Protection*, *93*, 154–160. https://doi.org/10.1016/j.psep.2014.03.002

Tekin, K., Karagöz, S., & Bektaş, S. (2014). A review of hydrothermal biomass processing. *Renewable and Sustainable Energy Reviews*, *40*, 673–687. https://doi.org/10.1016/j.rser.2014.07.216

Tran, K.-Q. (2016). Fast hydrothermal liquefaction for production of chemicals and biofuels from wet biomass – The need to develop a plug-flow reactor. *Bioresource Technology*, *213*, 327–332. https://doi.org/10.1016/j.biortech.2016.04.002

Valderrama Rios, M. L., González, A. M., Lora, E. E. S., & Almazán del Olmo, O. A. (2018). Reduction of tar generated during biomass gasification: A review. *Biomass and Bioenergy*, *108*, 345–370. https://doi.org/10.1016/j.biombioe.2017.12.002

Vassilev, S. V, Baxter, D., Andersen, L. K., Vassileva, C. G., & Morgan, T. J. (2012). An overview of the organic and inorganic phase composition of biomass. *Fuel*, *94*, 1–33. https://doi.org/10.1016/j.fuel.2011.09.030

Wang, T., Zhai, Y., Zhu, Y., Li, C., & Zeng, G. (2018). A review of the hydrothermal carbonization of biomass waste for hydrochar formation: Process conditions, fundamentals, and physicochemical properties. *Renewable and Sustainable Energy Reviews*, *90*, 223–247. https://doi.org/10.1016/j.rser.2018.03.071

Yang, W., Li, X., Li, Z., Tong, C., & Feng, L. (2015). Understanding low-lipid algae hydrothermal liquefaction characteristics and pathways through hydrothermal liquefaction of algal major components: Crude polysaccharides, crude proteins and their binary mixtures. *Bioresource Technology*, *196*, 99–108. https://doi.org/10.1016/j.biortech.2015.07.020

Yedro, F. M., García-Serna, J., Cantero, D. A., Sobrón, F., & Cocero, M. J. (2014). Hydrothermal hydrolysis of grape seeds to produce bio-oil. *RSC Advances*, *4*(57), 30332–30339. https://doi.org/10.1039/C4RA00429A